POLITECNICO DI TORINO

Corso di Laurea Magistrale in Ingegneria Aerospaziale

Interface Reduction in Component of Bladed Disks by Different Methods

October 6, 2019

Supervisors:
Prof. Botto Daniele
Prof. Urlapkin Aleksandr

Candidate:
Mr. Scarso Stefano

"Dedicated to my parents"

Thesis Acknowledgement

I would like to thank my family: my parents Maria and Patrizio for the economical and motivational support during these years of studies. I want to thank also Giancarlo for the motivation during difficulties. During these years they were the safe port and a beacon of hope.
I would like to express my sincere gratitude to my supervisors Prof. Botto Daniele and Prof. Urlapkin Aleksandr for the continuous support given during my master's thesis research, for their patience and enthusiasm. I would like to express my sincere gratitude to Prof. Vinogradov Alexander, responsible of my exchange programme in Samara University, for all the support and encouragement given during the year spent in Russia. I want to thank all my classmates to let me spent beautiful moments in Turin during the periods of lesson. In particular I want to thank: Cavallera Ilario, Giusa Daniel, Favalli Federico for the support given as colleagues and friends. I want to thank Orlando Giulio for sharing with me the beautiful experience spent in Russia. I want to thank my friends: Coronese Alberto Luigi, Zampollo Paolo, Tria Sara, Lombardi Marco, Becce Lorenzo and Manconi Francesco for the motivation given during these years of university in Turin. I want to thank all the members of the student's association AESA Torino for all the knowledge taught.
I wish to all the people that supported me during these five years good luck and a life full of success.

Я бы очень хотел выразить благодарность всем моим друзьям из Самары, которые помогали мне, когда я жил в России. Также, я бы хотел поблагодарить мою девушку, Мустафину Данию, которая помогала мне, помогает до сих пор, и продолжает этот путь вместе со мной. Также, хотелось бы сказать «спасибо» ребятам из AEGEE Samara. Вы все - мои друзья! Вы помогли мне устоять перед трудностями, я очень много учился и всё получилось. Данная диссертация посвящена, в том числе, и вам. Я желаю всем счастья и попутного ветра!
Спасибо!

List of Figures

List of Tables

Contents

1 Introduction

This thesis work has the aim to study a rotor disk of a compressor for aeronautical applications. It's known, that if a rotor disk of a compressor is considered, from a failure point of view, the blades are the most critical component. The main cause derives mostly from vibrations generated from external forces. This phenomenon it's cause of a reduction of the time to failure of the compressors. In this thesis, first some theory about systems of compressor and mistuning is given. This helps to understand the dynamic behaviour of a rotor disk and how it changes when the geometry of the disk is slightly different from the nominal one and cannot be modelled under cyclic symmetry conditions. Deviation of the disk's geometry from the nominal one is known to us as "Mistuning". More simply, mistuning means that the rotating disk is not perfectly symmetric along the rotation axis. To study the effects of mistuning on the dynamic behaviour of the disk first an approximation of the system is needed. This task is very demanding because it depends on many factors and some of them are difficult to predict. In this work a "Full disk model" geometry has been developed with a two degrees of freedom (DoF'S) per sector. In this model, all the sectors of the rotor wheel have been considered and modelled. After this, a "Sector cyclic model", made with only one disk sector of three degrees of freedom (DoF's) then reduced to two, has been developed. It's better to specify that one sector comprehends a slice of disk and one blade. For this reason, the number of sectors will be always equal to the number of blades. The "Sector cyclic model" it's simpler than the "Full disk model" because it considers only one sector instead of all of them. Dynamic results from the "Full disk model" (the benchmark) and from the "Sector cyclic model", under appropriate model and calculus assumption, have been compared. The aim of the comparison is to check if dynamic analysis performed on a single sector are reliable and gives dynamic response with enough degree of accuracy. Since a model of two degrees of freedom (DoF's) per sector it's too approximative, another system of twenty-four blades disk is developed with the help of the software ANSYS. This model will be the benchmark for the further steps. The goal of this second part is to investigate about the possibility to find a reduced model of the disk that can approximate the study of a rotor wheel without mistuning. In this manner it will be possible to study the full model considering few nodes. These nodes are called “master nodes”. The reduction of the number of nodes has been done on the interfaces between the sectors of the disk. This reduction was done with the help of some shape functions obtained with different methods. These methods are respectively; SEREP (System equivalent expansion reduction process), Four-noded rectangular element reduction, Eight-noded rectangular element reduction and Nine-noded rectangular element reduction. In the conclusions it’s shown which methods better approximate the results obtained from the model developed on ANSYS. The results of this work could be than used to study a rotor wheel in presence of mistuning.

1.1 Explanation of the sections of the thesis

This work is divided into three parts. The first part, that comprehends respectively chapter 2 and chapter 3, gives some basic theory about the dynamic behaviour of a bladed disk and the calculation of natural frequencies with and without external force. The aim of this first part is to understand properly how it's possible to describe through graphs and numbers the behaviour of a bladed disk under certain working conditions. Another aim of this part is to explain and demonstrate the advantages of considering a "Sector Cyclic model" instead of a "Full disk model".
The second part has the aim to propose some reduction methods to decrees the number of nodes on the interfaces between the sectors of the disk. In this manner it's possible to study the same system but with a reduced number of degrees of freedom (DoF's). The big advantage to do so is the smaller quantity of data that have to be managed. The third part, in the appendices, comprehends a general and basic view of mistuning and his effects on the final results of a bladed disk. This last part gives the possibility to use the conclusions obtained in the second part applying them on a mistuned rotor wheel.

2 Dynamics of Bladed Disk without external forces

2.1 Basic theory of disk and Nodal diameter

A bladed disk or rotor wheel is a component of the turbo-machine which consists of two main parts, a disk and blades attached on it. These components, when are designed and defined on the software, are characterized by a perfect cyclic symmetry around the rotation axis.
To make things more understandable, the bladed disk could be considered as a membrane. This membrane under certain working conditions will displace from the original plane. To every point of the bladed disk will be associated a displacement. Of course, it's an initial approach that makes the physical meaning more understandable in every configuration in which the system vibrates.

Figure 2.1.1: Example of rotor wheel or bladed disk

In Figure 2.1.1 it's shown a rotor wheel built with the blisk technology. This kind of technology consists of just one part, instead of an assembly of a disk and individual blades.
In general the main concept of this paragraph is that during each working operation of the engine, the rotor wheels will vibrate with a specific frequency. This vibration will produce displacements of every point of the disk except of the one along the nodal diameter. With the term "`nodal diameter`"

it's meant a group of points called "`nodes`", in which the value of the displacement from the original plan is equal to zero. There are several nodal diameters and each of them corresponds to a particular value of frequency. In

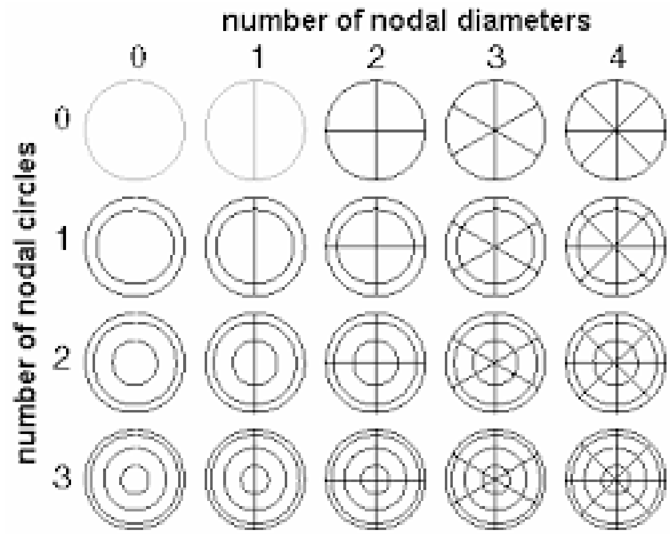

Figure 2.1.2: Table of Nodal diameters and circles

Figure 2.1.2 it's possible to see that also "`nodal circles`" exist.They have the same explanation of "`nodal diameters`" but instead of having a linear geometry they have a circular one. In this thesis the work will be focused only on "`nodal diameters`". The main concept is that more the frequency is increased and more diameters will occur on the disk. This concept could be explained with the help of the following figure.

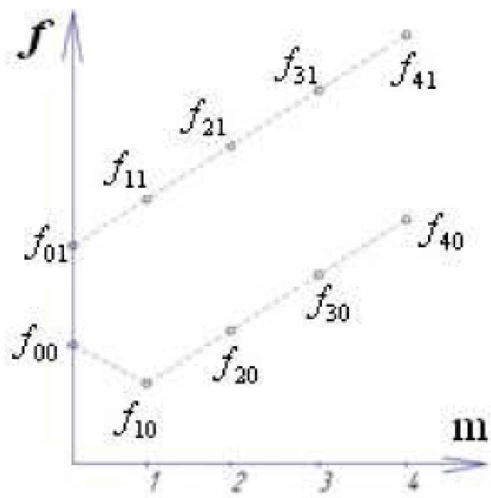

Figure 2.1.3: Spectrum of rotor wheel vibration

The symbol f_{01} refers to the frequency in which zero nodal diameters and one circular diameter occur. The same will be with the other ones. In Figure 2.1.3 it's possible to see that if "m" (number of nodal diameters) it's increased, the frequency increases too.
The number of nodal diameters is also strictly connected to the number of sectors of the evaluated component.
In order to simplify our studies, the sector will always comprehend a blade and the correspondent slice of disk body. In this way the opening angle (A) of the slice of disk will be equal to:

$$A = \frac{360}{N}$$

Where N is the number of blades.
Once we defined the number of sectors, that is equal to the number of blades, we can find the correlation between the number of nodal diameters (n) and the number of sectors (N) in the following way.

- $0 \leq n \leq \frac{N}{2}$ if N is even
- $0 \leq n \leq \frac{N-1}{2}$ if N is odd

2.2 Modelling of the Full Disk Model

In this chapter an approximation of the disk and blade with the Full Disk Model it's built to develop the main mathematical equations.

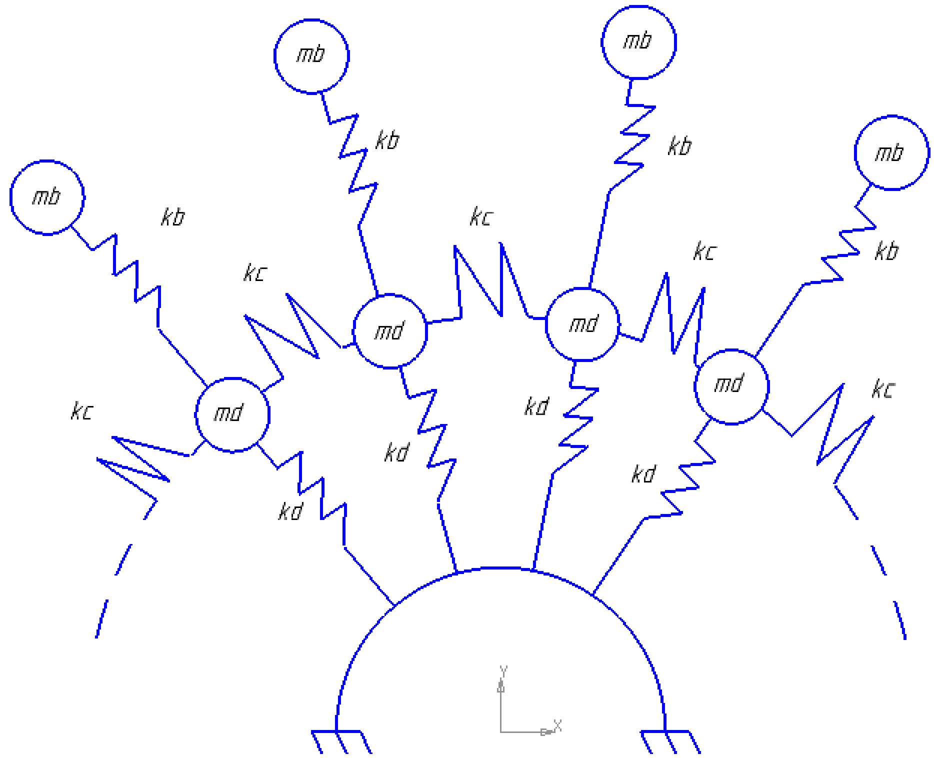

Figure 2.2.1: Complete system

In 2.2.1 it's shown the approximation considered. It's visible that there are two types of mass; the mass of the disk (m_d) and the mass of the blade (m_b). We have also three types of stiffness, respectively stiffness of the blade (k_b), the stiffness of the disk (k_d) and the stiffness of the connection part (k_c).
It's possible to understand visually that every sector has two DOF's (degrees of freedom). Another approximation is that all the distributed mass of the disk and blades are been simplified in point like masses. The equation needed to solve the system is the following:

$$[M]\{\ddot{X}\} + [K]\{X\} = \{0\} \tag{2.2.1}$$

The Equation 2.2.1 calculates the solutions of the system.
In the next pages the letter "N" represents the number of sectors of the

complete structure.
In this analysis, as already said, two DOF's for each sector are considered. The vector $\{x\}$ represents the physical displacement coordinates of dimension $2N \times 1$ and [M] and [K] respectively the mass and stiffness matrix of dimension $2N \times 2N$.
To better understand how this two matrices are built, it's necessary to decide the order of the displacements variables. Each degree of freedom will have his proper displacement. The degrees of freedom are ordered as it follows.

$$\{X\} = x_i$$

where x_i is the displacement of the i-th mass, it could be both mass of the blade or of the slice of the rotor wheel. In this case, the following numeration system has been given.

- i ∋ [1,N], degrees of freedom of the slices of the rotor wheel.
- i ∋ [N+1,2N],degrees of freedom of the blades.

It follows a more precise explanation of how the mass matrix [M] and the stiffness matrix [K] are built. [M] matrix is an all zero matrix except in the main diagonal where in the first N-elements the values are all equal to the disk mass and from element N+1 to 2N the mass of the blades. It follows a representation of this matrix.

$$[M] = \begin{bmatrix} m_d & 0 & ... & ... & ... & 0 \\ 0 & m_d & ... & ... & ... & 0 \\ ... & ... & ... & ... & ... & ... \\ 0 & 0 & ... & ... & m_b & 0 \\ 0 & 0 & ... & ... & ... & m_b \end{bmatrix}$$

As already said the dimension of [M] is $2N \times 2N$.

For the construction of the [K] matrix, an assembly method similar to the one used to assembly nodes in FEM techniques has been used. The first step is to generate the three local matrixes for the stiffness. They are the following:

$$[K_c] = \begin{bmatrix} k_c & -k_c \\ -k_c & k_c \end{bmatrix}$$

$$[K_b] = \begin{bmatrix} k_b & -k_b \\ -k_b & k_b \end{bmatrix}$$

$$[K_d] = \begin{bmatrix} k_d & -k_d \\ -k_d & k_d \end{bmatrix}$$

With respectively $[K_c]$, $[K_b]$ and $[K_d]$ the local matrixes of connection, blade and slice of the disk. Furthermore a numerical order to the degree of freedom was given. In the case of study the order of the DOF's related to the slice of disk was starting from 1 to N. The order of the DOF's for the blades is starting from N+1 and ending with 2N. In figure 2.2.2 is given a visual example of this numerical order.

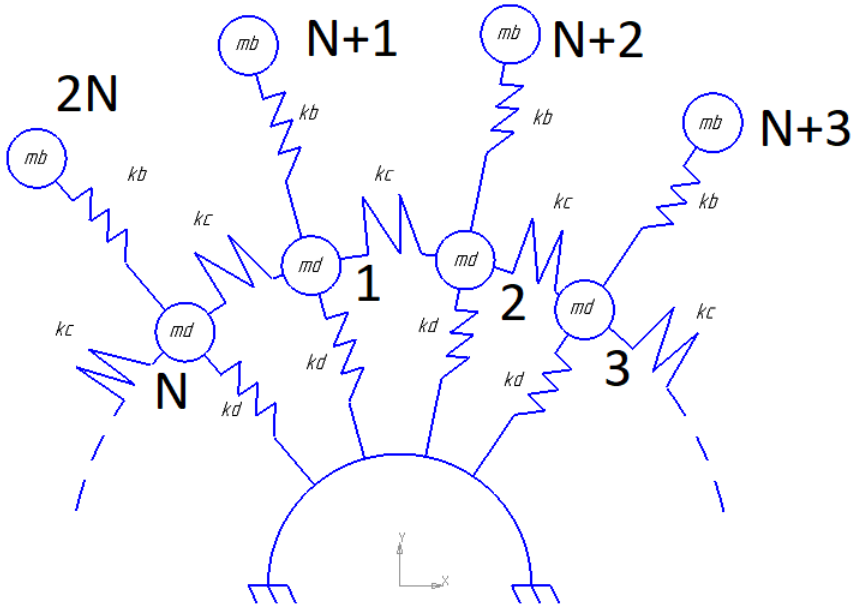

Figure 2.2.2: Order of the nodes for the complete system

In this way it's possible to build the global stiffness matrix [K] by assembling the three local matrixes by considering the order number.
As the global mass matrix [M], the stiffness matrix [K] is of dimension $2N \times 2N$.
To better understand this assembly process an example of a system of 4 sectors is reported. The order of the numbers will be, from 1 to 4 for the DOF's of the slice of disk and from 5 to 8 for the DOF's of the blades. The global stiffness matrix [K] of such a system is the following:

$$[K] = \begin{bmatrix} k_s & -k_c & 0 & -k_c & -k_b & 0 & 0 & 0 \\ -k_c & k_s & -k_c & 0 & 0 & -k_b & 0 & 0 \\ 0 & -k_c & k_s & -k_c & 0 & 0 & -k_b & 0 \\ -k_c & 0 & -k_c & k_s & 0 & 0 & 0 & -k_b \\ -k_b & 0 & 0 & 0 & k_b & 0 & 0 & 0 \\ 0 & -k_b & 0 & 0 & 0 & k_b & 0 & 0 \\ 0 & 0 & -k_b & 0 & 0 & 0 & k_b & 0 \\ 0 & 0 & 0 & -k_b & 0 & 0 & 0 & k_b \end{bmatrix}$$

In Equation 2.2.1 no external forces are applied, for this reason the damping matrix [C] is not considered. It is also known that these kinds of linear differential equations admit solution as it follows:

$$\{X\} = \{X_0\}cos(\omega t + \theta) \tag{2.2.2}$$

with $\{X_0\} \ni R^n$.

By taking, then, the first and the second derivative in the time domain of the coordinates $\{X\}$, it is possible to insert them in equation 2.2.1 obtaining the following system of equation.

$$([K] - \omega^2[M])\{X_0\} = 0 \tag{2.2.3}$$

The non trivial solution is the one that must be considered as it follows.

$$det([K] - \omega^2[M]) = 0 \tag{2.2.4}$$

It's possible then to solve the characteristic equation 2.2.4 which represents the eigenvalues. On the diagonal of the matrix of the eigenvalues it's possible to find the natural frequencies $(\omega)_i$ where the subscript (i) goes from 1 to 2N. For this reason, the matrix of eigenvalues will be of dimension $2N \times 2N$. In case of a tuned rotor wheel, this mean that that disk is perfectly symmetric along the rotation axis, the $2N$ frequencies will be in couples. This result comes from the property of symmetry. There is only an exception in the first and last frequency that will not be in couple. An example of the first frequencies obtained in the case of study is reported in the following table. In this table some values of frequencies with an increasing order are reported for a bladed disk with a number of sectors (N) equal to 50, a disk mass $m_d = 1.5Kg$ and a blade mass to $m_b = 0.5Kg$. The frequencies for disk, connection and blade are respectively $k_d = 300Hz$, $k_c = 300Hz$ and $k_b = 100Hz$.

Frequencies [Hz]	Mode shape number
97.9893	1st shape mode
98.023	2nd shape mode
98.023	3th shape mode
98.1172	4th shape mode
98.1172	5th shape mode
98.2544	6th shape mode
98.2544	7th shape mode
98.4138	8th shape mode
98.4138	9th shape mode
98.5774	10th shape mode
98.5774	11th shape mode
98.7329	12th shape mode
98.7329	13th shape mode
...	...

Table 2.2.1: Calculated frequencies by increasing order with related shape modes for a full disk model of two DoF's per sector

In order to visualize the mode shapes for different natural frequencies we used the matrix of eigenvectors. This matrix represents the displacement of the DOF's for a certain frequency. With this values it's possible to build the following diagrams reported in Figure 2.2.3 and 2.2.4. In these diagrams it's possible to see the and understand the displacement for every DOF of the disk. In these diagrams the 50 sectors rotor wheel is evaluated.

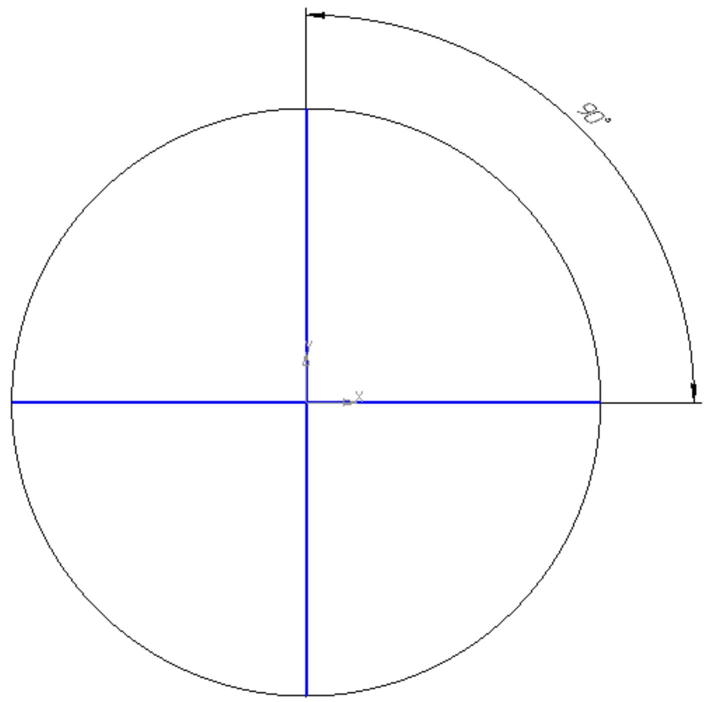

Figure 2.2.3: Rotor wheel (only) with two nodal diameters

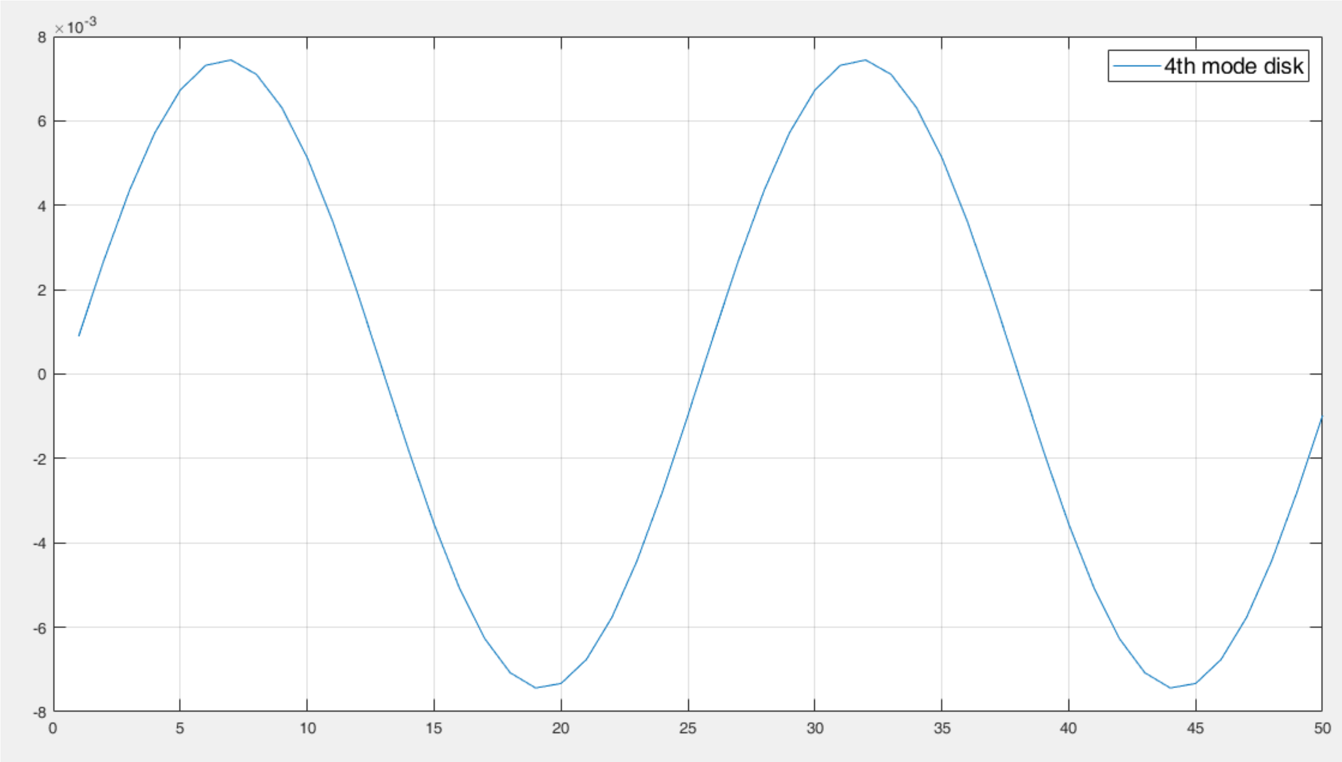

Figure 2.2.4: 4th mode shape displacement diagram

In Figure 2.2.4 it's possible to see the typical $4th$ mode shape for the disk. In this case, is visible the presence of two nodal diameters (the curve intersect the x axis four times). To explain this concept in a proper way it's better to start from the geometry of a bladed disk like shown in Figure 2.2.3. In this diagram two nodal diameters are represented, it means that along this lines the amplitude of the displacements is equal to zero. By taking a look along the external circumference of the disk (the border) it's possible to see that this curve meet the nodal diameters four times. In this case, on the first sector (0°) or equal to 12 o'clock, the displacement is zero (due to the correspondence with a nodal diameter). It's possible to see the same in Figure 2.2.4. The same theory could be applied for the sectors in correspondence with (90°),(270°) and again (360°).
Since from the matrix of eigenvalues we get couple of frequencies, as already showed in the table of the frequencies, it means that there are couples of shape modes that have the same frequency but have a different phase angle. With the help of Figure 2.2.5 and 2.2.6 it's easier to explain this concept.

It is also visible in Figure 2.2.6 that the nodal diameters for the 4th and the 5th mode shape are shifted of 45°. This angle, called phase angle, is obtained mathematically by the half of the angle between two nodal diameters. Since in the 4th mode shape occur two nodal diameters perfect orthogonal, the angle between them is 90°. This angle is shown in Figure 2.2.3. To obtain the phase angle between two shape modes with the same frequency it's necessary to divide this angle by two.

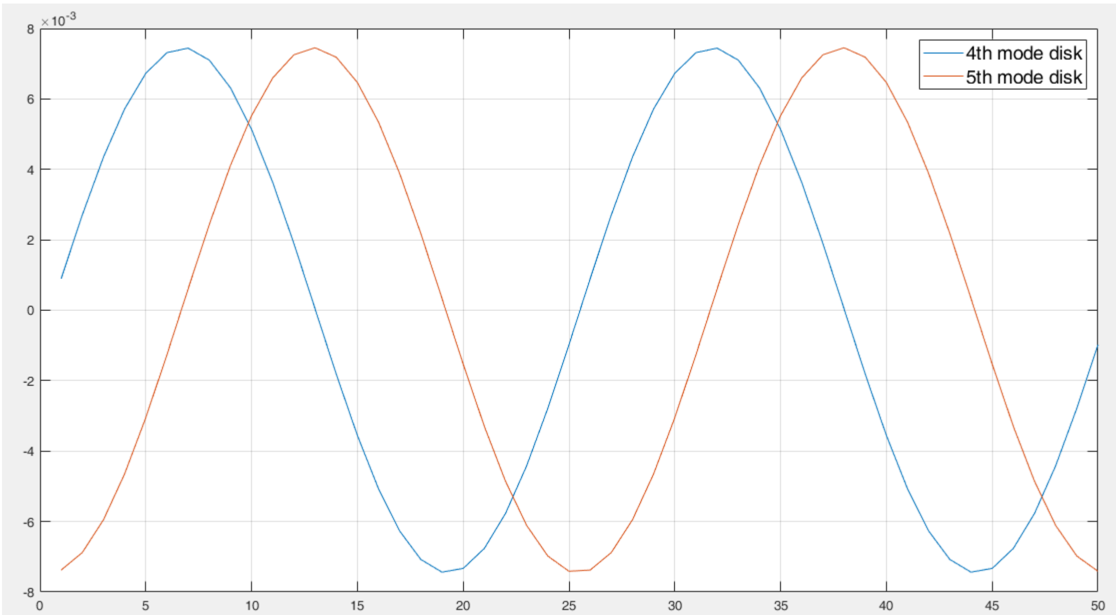

Figure 2.2.5: 4th and 5th shape mode comparison complete system

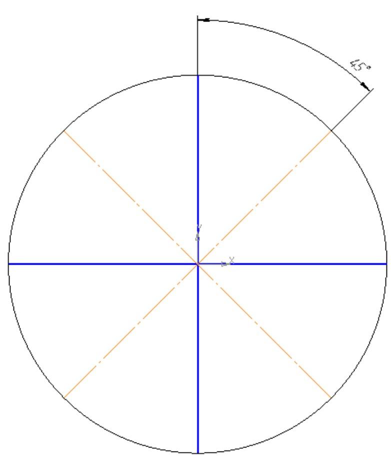

Figure 2.2.6: 4th and 5th shape mode comparison on disk for complete system

It's possible to do the same for higher frequencies. In the following figures are shown the comparison of the shift angle between the 8th - 9th and 12nd - 13rd shape mode.

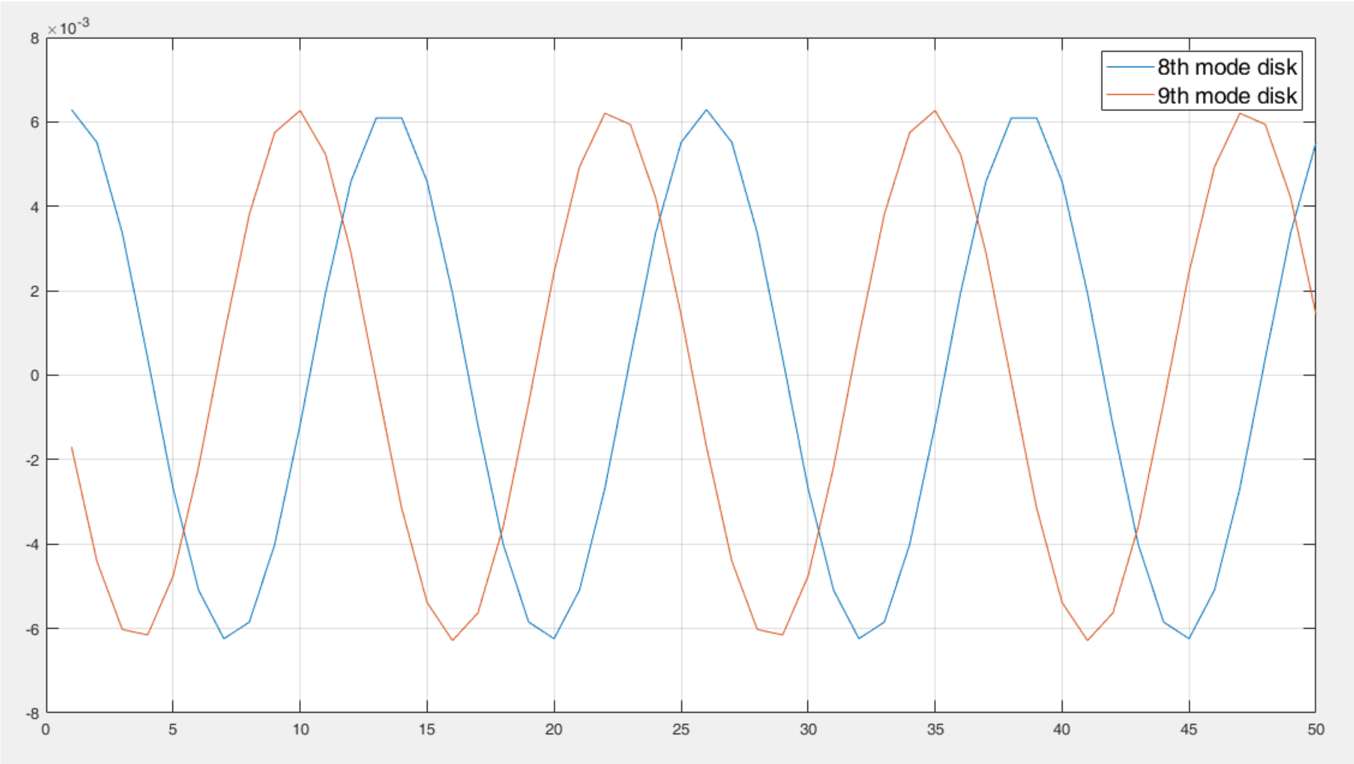

Figure 2.2.7: 8th and 9th shape mode comparison complete system

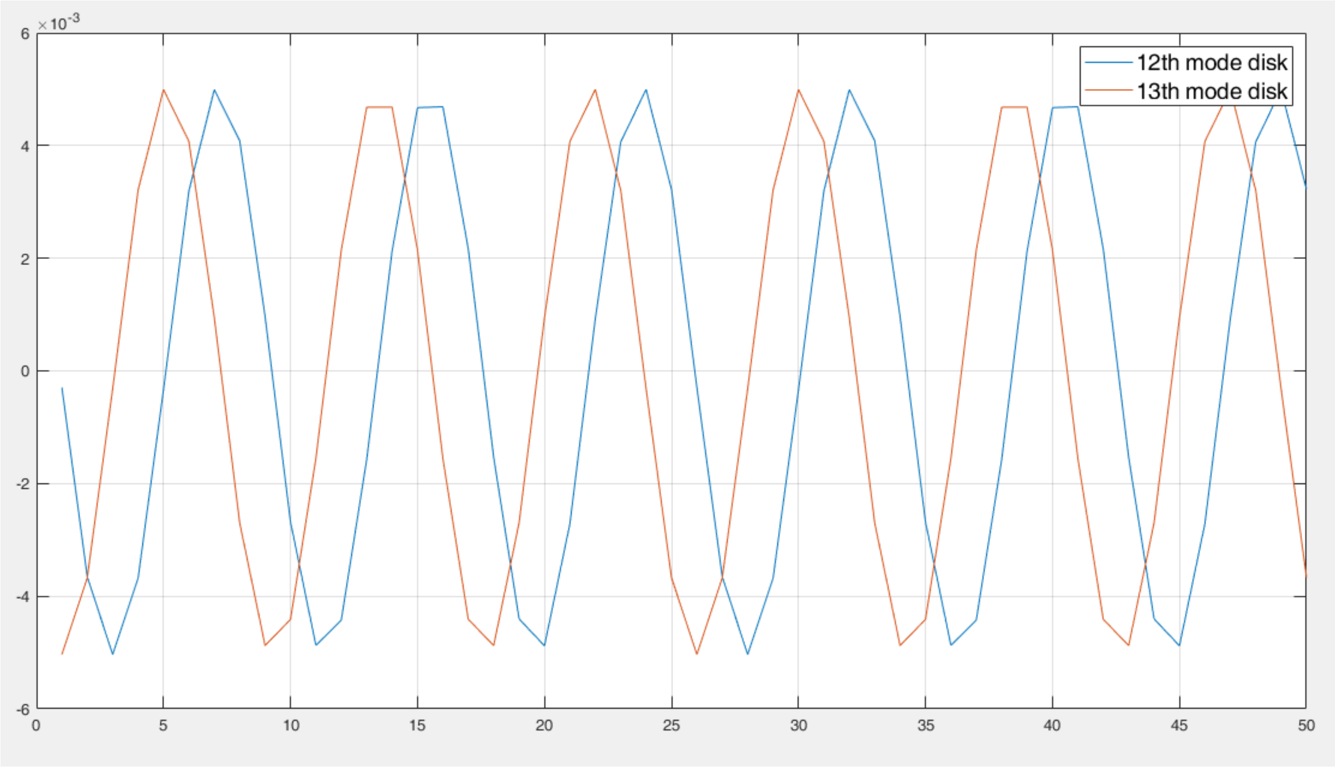

Figure 2.2.8: 12nd and 13rd shape mode comparison complete system

If the 8th and the 9th shape modes are considered, it's possible to see that the number of nodal diameters will be equal to four. For this reason the angle between the diameter in the 8th shape mode will be equal to 45°. The phase angle between the 8th and the 9th shape mode will be 22.5°.
It's also visible in the previous diagrams, Figure 2.2.7 and 2.2.8, that more we increase the frequency and more the shape of the curve appears less smooth. This reason comes from the choice of the number of sectors. In the previous study the number of sectors (N) is equal to 50. If this number it's increased for example to 150, it's possible to obtain a smoother mode shape. In this first study a small number of sectors was chosen not to perform big calculations.

2.3 Modelling of the cyclic symmetry structure

In this chapter an approximation of the slice of the rotor wheel and the blade with the Sector Cyclic Model it's built. In general it's possible to say that a tuned bladed disk satisfies the property of cyclic symmetry along the rotation axis. This property could be used to study the disk's dynamics, reducing a lot the steps to compute big systems of data with many degrees of freedom and sectors. The aim is to build a model that satisfies the property of symmetry to be able to focus the attention only on one sector. This sector then, with the help of the phase angle, will be repeated to reproduce all the sectors of the complete disk. In this way, the process of calculation will be shorter and easier. Among the various types of systems, a sector model is defined we three degrees of freedom (DOFs) respectively for the three masses.

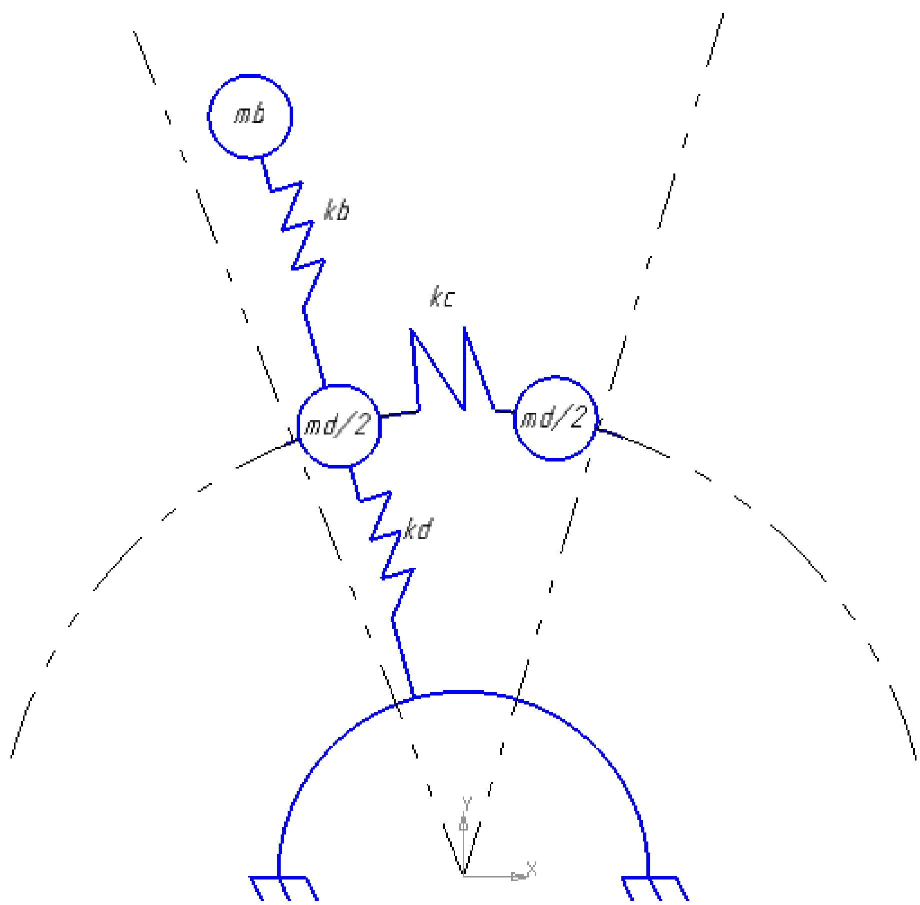

Figure 2.3.1: Sector cyclic model

For reasons connected to symmetry, the mass of the slice of the rotor wheel has been divided into two half masses.
For this new system, a new displacement's vector {x} must be created as it follows:

$$\{x\} = \{x_{d,l}, x_b, x_{d,r}\}$$

Where:

- $x_{d,l}$ is the coordinate for the left slice of rotor wheel mass
- $x_{d,r}$ is the coordinate for the right slice of rotor wheel mass
- x_b is the coordinate for the blade mass

By doing a comparison between the Full Disk Model and the Sector Cyclic Model it's possible to see that in the first model the degrees of freedom (DOF's) of one sector were two. In this new model the number of degrees of freedom (DOF's) are three. In the following pages a way to link the DOF of the right mass of the disk and the DOF of the left mass of the disk will be explained. By doing so the DOF's will be two as in the Full Disk Model.

Once generated the coordinates system, mass matrix $[M_s]$ and stiffness matrix $[K_s]$ must be found in the following way.

$$M_s = \begin{bmatrix} \frac{m_d}{2} & 0 & 0 \\ 0 & m_b & \frac{m_d}{2} \\ 0 & 0 & \frac{m_d}{2} \end{bmatrix}$$

$$K_s = \begin{bmatrix} k_d + k_c + k_b & -k_b & -k_c \\ -k_b & k_b & 0 \\ -k_c & 0 & k_c \end{bmatrix}$$

To solve the system it's necessary to find the solution to the following equation.

$$[M_s]\ddot{X} + [K_s]X = 0 \tag{2.3.1}$$

Until now, still no information about the other of the sectors has been introduced. First, as already explained in the previous page, the system needs an equation that connects the degree of freedom (DoF) of the left disk mass with the one of the right mass. This could be done by introducing a phase angle $\{\mu\}$ calculated by Equation 2.3.2

$$\mu = +\frac{2\pi}{N}n \tag{2.3.2}$$

Where:

- N is the number of sectors
- n is the number of nodal diameters that we want to study n = $[0,...,\frac{N}{2}]$ and N even number

In this way is possible to built the complex constrains able to reduce the number of degrees of freedom from three to two. The new coordinate system {x'} will be as it fallows.

$$\{x_{d,r}\} = e^{i\mu}\{x_{d,l}\}$$

$$T = \begin{bmatrix} 1 & 0 \\ 0 & 1 \\ e^{i\mu} & 0 \end{bmatrix}$$

The new system of coordinates $\{x'\}$ will be defined as it follow:

$$\{x'\} = \{x_{d,l}, x_b\}^T$$

In this case new matrixes of dimension 2×2 are developed:

$$M_s'(\mu) = [T]^T[M_s][T]$$

and

$$K_s'(\mu) = [T]^T[K_s][T]$$

By replacing this new matrixes in Equation 2.3.1 it's possible to obtain the following system's equation:

$$[M_s'(\mu)]\ddot{X'} + [K_s'(\mu)]X' = 0 \tag{2.3.3}$$

It's possible then to solve this equation and obtain the eigenvectors matrix $[\psi(\mu)]$ of dimension 2×2. For a comparison with the eigenvectors matrix of the complete system further steps must be done.

First a transformation matrix $[T_{\psi_s}]$ should be developed in the following way:

$$[T_{\psi_s}] = \begin{bmatrix} \dots \\ e^{ik\mu}[I] \\ \dots \end{bmatrix}$$

Where $[I]$ is the Identity Matrix 2X2 and the index $k = 0, ..., N-1$.
It's possible then to obtain the matrix of eigenvectors for the cyclic system expanded $[\psi_{exp}(\mu)]$:

$$[\psi_{exp}(\mu)] = [T_{\psi_s}][\psi(\mu)]$$

The eigenvectors contained in the expanded matrix $[\psi_{exp}(\mu)]$ are complex. It is then experimentally verified that they have a phase angle respect to the fully study system.

3 Dynamics of Bladed Disk with external force

In this Chapter the same steps of Chapter 2 will be followed. The system will be studied both in Full Disk Model and Sector Cyclic Model with an additional external force. For this reason, in the main equation of the system, a study of a damping matrix it's also necessary. In the following studies a force will be applied on the blades of the rotor wheel. This force is generated by the flow that passes through the blades of the compressor. It's known that this force creates a tangential component (R_a) and an axial component (R_u). There is also a radial force but in this picture is not shown for simplifying reasons. This concept is shown in Figure 3.0.1

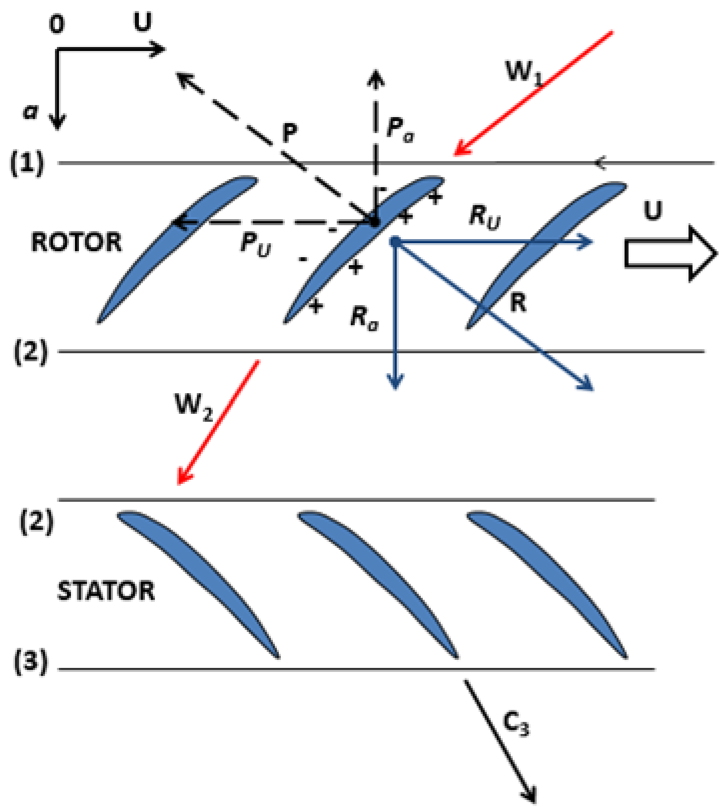

Figure 3.0.1: Components of the force applied on the blade

To simplify the study, only the tangential component (R_u) is considered, as shown in Figure 3.0.2.

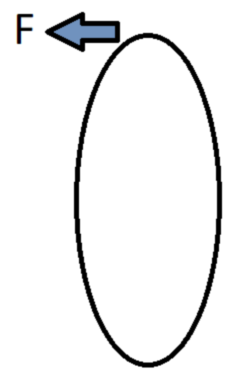

Figure 3.0.2: Disk with external force (F) applied

Through the blades the Force (F) applied on the blades will stress also the disk. For this reason, as shown in Figure 3.0.2, the force is applied on the circumferential part of the disk. The direction of this force is the same of the springs of the model. It means that if we choose tangential displacements, and for this reason we consider the direction of the springs that simulate the stiffness of the material tangential, the force component that we consider is the tangential one. The same concept could be applied to the axial and the radial component. Anyway this choice doesn't change our calculation.
F is expressed by the following equation:

$$F = F_0 sin(\omega t) \tag{3.0.1}$$

where ω is the excitation frequency and Ω is the rotational frequency of the disk. This external force is given by the interaction between the gases entering in the compressor. The fact that this force is transmitted from the gas by the rotation of the rotor wheel allows that this force could be considered as a "Rotation Force". The excitation frequencies that make resonance occurs are multiple directly with the rotational speed of the rotor wheel. In literature, this concept is described by a value called Engine Order. The engine order (EO) expresses the ratio between the excitation frequency and force. This is not completely true because the interaction between the gas fluxes and the blades is impulsive. Anyway, a Fourier series study can be operated to deal with harmonic functions. The Engine Order (EO), is defined by $EO = \frac{\omega}{\Omega}$. This value can be also obtained by $EO = N \pm n$ where N is the number of

sectors and n is the nodal diameter. The Engine Order, defined in this way, is meant to excite, in resonance condition, a mode associated to a specific nodal diameter. In the previous equations this concept is mathematically shown. A mode with nodal diameter n can be excited by an Engine Order having the same value but also by an Engine order equal to $N \pm n$. The cause of this last concept is linked with the "aliasing phenomenon". In this case, the rotation of the bladed disk, considering that the blades are not continuous because they are equally spaced, causes a sampling effect of the harmonic forcing function. When the EO is bigger than $\frac{N}{2}$ the sampling of this forcing signal is not considered "correct". It means that the disk can't see such excitation force but it sees a force with a lower excitation frequency. Then, each blade, undergoes the same excitation force in terms of amplitude but with a phase lag that depends on the position of the blade.
The excitation force vector F acting on the blades, in the rotating reference frame fixed to the disk, can be written as it follow.

$$\{F\} = \overline{\{F_0\}} e^{i\omega t} and \overline{\{F_0\}} = \{F_0\} e^{i\phi m} \tag{3.0.2}$$

Where:

- $\{F_0\}$, is amplitude vector of the forcing function (F_0 is a real number)
- ϕ , inter-blade phase angle ($\phi = \frac{2\pi}{N} n = \frac{2\pi}{N} EO$)
- m, position number of the blade ($m = 1, ..., N$)

3.1 Modelling of the complete structure with external force applied

In order to evaluate the forced response of the complete system, a damping matrix [C] has to be calculated. For simplicity we consider a proportional viscous damping. This allows us to build the damping matrix by fixing a value of modal damping ratio ζ_c for each mode.

$$[c_r] = diag(2\zeta_c \sqrt[2]{k_r m_r})$$

Where k_r and m_r are respectively the stiffness and the masses modal matrix. At this moment is possible to calculate the damping matrix [C] by the following equation.

$$[C] = ([\Psi]^T)^{-1}[c_r][\Psi]^{-1}$$

Where $[\Psi]$ represents the matrix of eigenvectors obtained from the system without external forces applied.

$$[M]\ddot{X} + [C]\dot{X} + [K]X = F \tag{3.1.1}$$

Then it's possible to solve the main equation 3.1.1.
First, it's possible to calculate a dynamic stiffness matrix

$$[K_{dyn}] = [K] - \omega^2[M] + i\omega[C]$$

and then use this matrix to solve the equation that can gives us the displacements.

$$X_0 = [K_{dyn}]^{-1}\overline{\{F_0\}}$$

It follows a forced response of the blades for a value of $EO = 1$ and $f = 98.023Hz$ (it means for one nodal diameter). The force, as already said is only applied on the blade's degree of freedom (DOF).

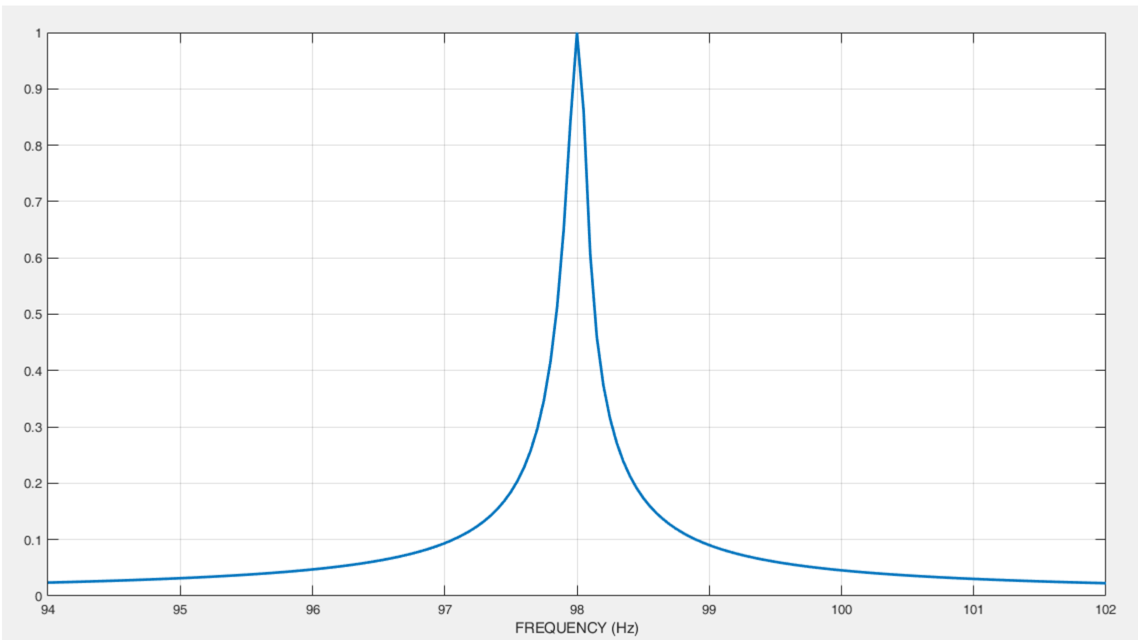

Figure 3.1.1: Forced response for the first nodal diameter

3.2 Modelling of the cyclic symmetry with external force applied

The forced response of the system can be also obtained by using the cyclic symmetry property. The excitation force is applied in the degree of freedom DOF of the blade. Through the phase ϕ, the continuity relation between the left side and the right one is established. It's possible to obtain the damping matrix in the same way as in the Full disk model. The step to follow are the same of the one followed in the Full disk model. The general equation of the system is:

$$Ms'(\mu)\ddot{X}' + Cs'(\mu)\dot{X}' + Ks'(\mu)X' = F_{0s}e^{i\omega t} \tag{3.2.1}$$

Being $\{x'\} = \{x_{d,l}, x_b\}^T$ the vector of the displacements.
In this vector it's possible to see the displacements for the blade and for the left slice of the mass of the disk. The amplitude force vector is then generated as $\{F_{0s}\} = \{0, F_0\}^T$.
The forced response can be computed through the inversion of the dynamic stiffness matrix, as in the case of the Full disk model. At the end it's possible to compare the Forced response diagram obtained with the Full Disk Model and the Sector Cyclic Model. In Figure 3.2.1, is shown a comparison of this two graphs. The comparison is done for the curve obtained with an $EO = 1$ and a frequency $f = 98.023Hz$.

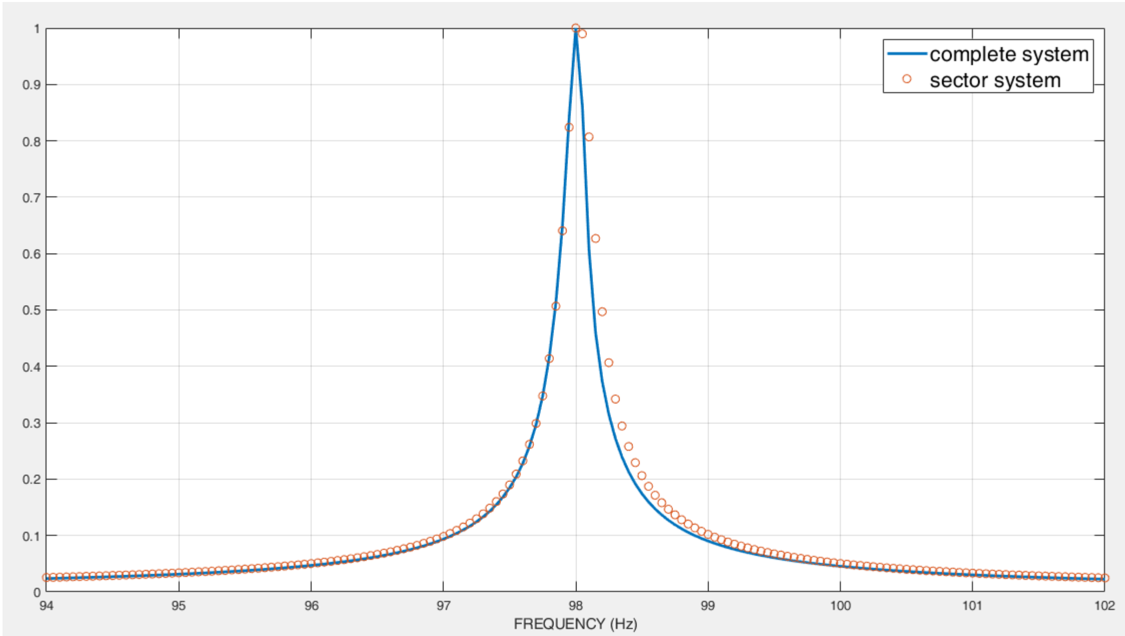

Figure 3.2.1: Forced response comparison between complete system and cyclic method for the first nodal diameter

It's possible to see from the forced response obtained by applying the two methods that the results are similar. For this reason, the previous chapters where used to demonstrate the capability of the Sector Cyclic Model to calculate a good approximation of the results obtained by a Full disk model. The advantages of this model is the simplicity. This characteristic is helpful to decrease the necessary time needed for calculation.

4 Modelling the "First reduced model" (FRM) of the disk

In the previous chapters the main theory behind the Mode shape analysis and the theory of Sector Cyclic Model where explained. It's easy to understand that both the models, Full disk model and Sector Cyclic model, with only two DOF's per sector, are a big approximation of a real bladed disk. It must be evaluated that is normal to evaluate several hundreds of nodes for one sector to obtain accurate results.

The big problem of such systems is the difficulty to manage and generate matrixes necessary to solve the model. This matrixes, due to the many DOF's per sector have large dimensions.

For this reason, in this chapter with the help of the software ANSYS a first reduction is done. This first reduction will create the "First reduced model". This simplification will keep only the nodes on the two contact faces of the sector and the nodes where the force (F) and reaction (R) are applied.

4.1 Generating the "First reduced model" (FRM) of one sector of the rotor wheel

A simple sector of a rotor wheel was designed with the help of the software NX 12.0 and then loaded on ANSYS. With the help of ANSYS then the mesh was built under constrains. The sector of the disk is designed to be part of a 24 sectors disk. In Figure 4.1.1 is reported the sector of the rotor wheel.

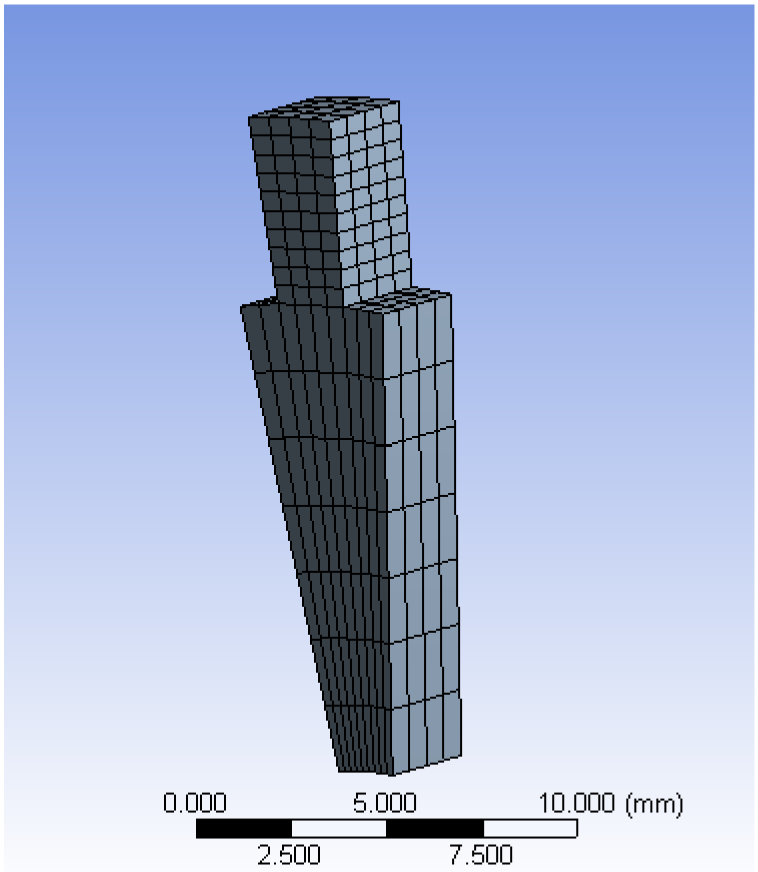

Figure 4.1.1: Sector of the simplified disk

An important characteristic that was required from mesh was that the coordinates of the nodes in the left face and in the right face were corresponded. This means that the coordinates of the nodes on the interfaces are perfectly coincident. This step was done in order to allow the assembly process, because even in this case, as done before the complete rotor wheel could be studied by only considering one sector that then will be repeated and translated with a phase angle. The efficiency of this method has been already

demonstrated in the previous chapters.
With the help of ANSYS it's possible to see the placement of the nodes created from the mesh. As it's possible to see in Figure 4.1.2 they are several hundreds.

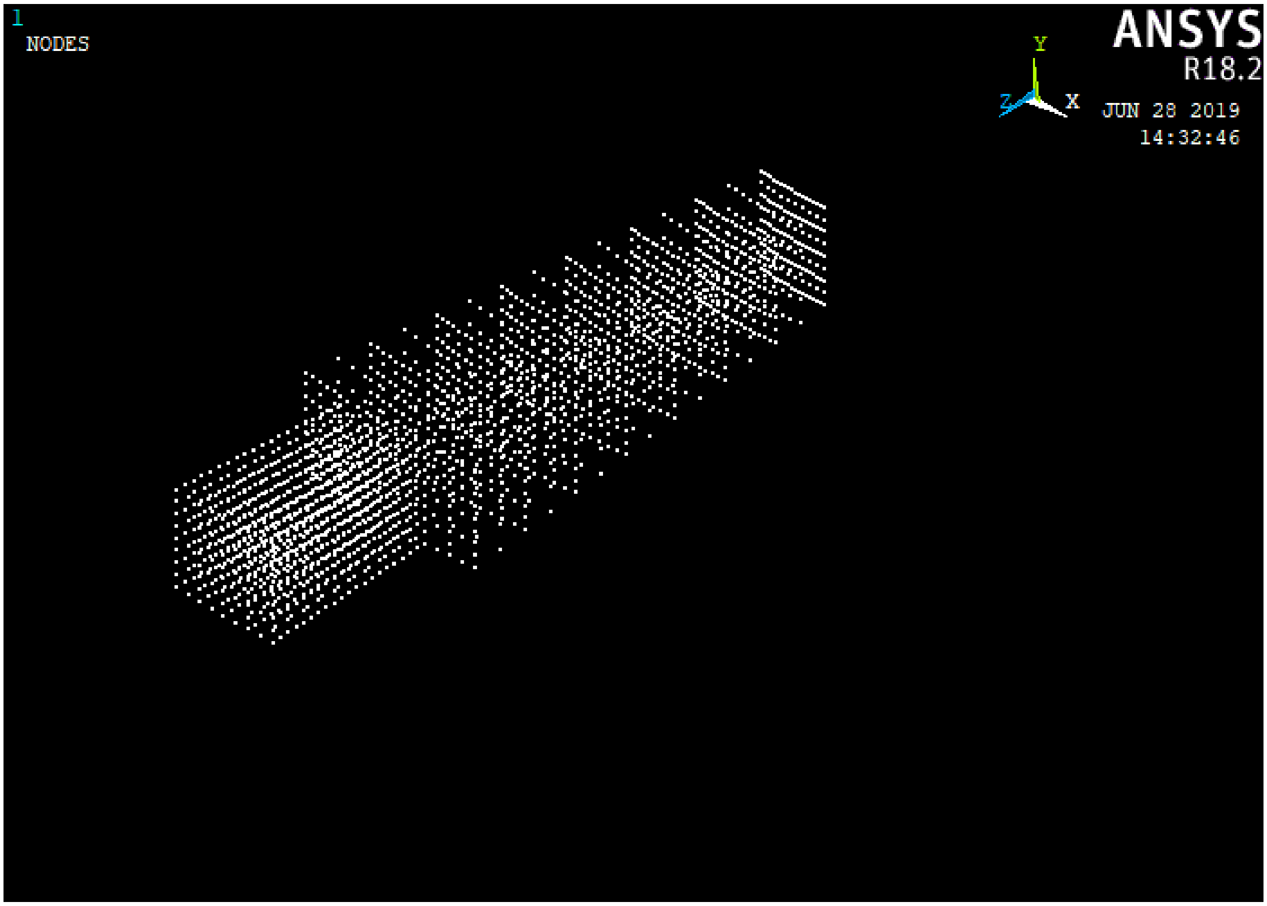

Figure 4.1.2: Nodes of the sector designed on ANSYS

In order to reduce the number of nodes, only the one placed on the connection surfaces (interfaces) and the two nodes where the force (F) and reaction (R) are applied were kept. For this reason four groups where selected. The first group of nodes is the one of the left contact surface. This group is shown in Figure 4.1.3. The second one is for the nodes on the right contact surface.

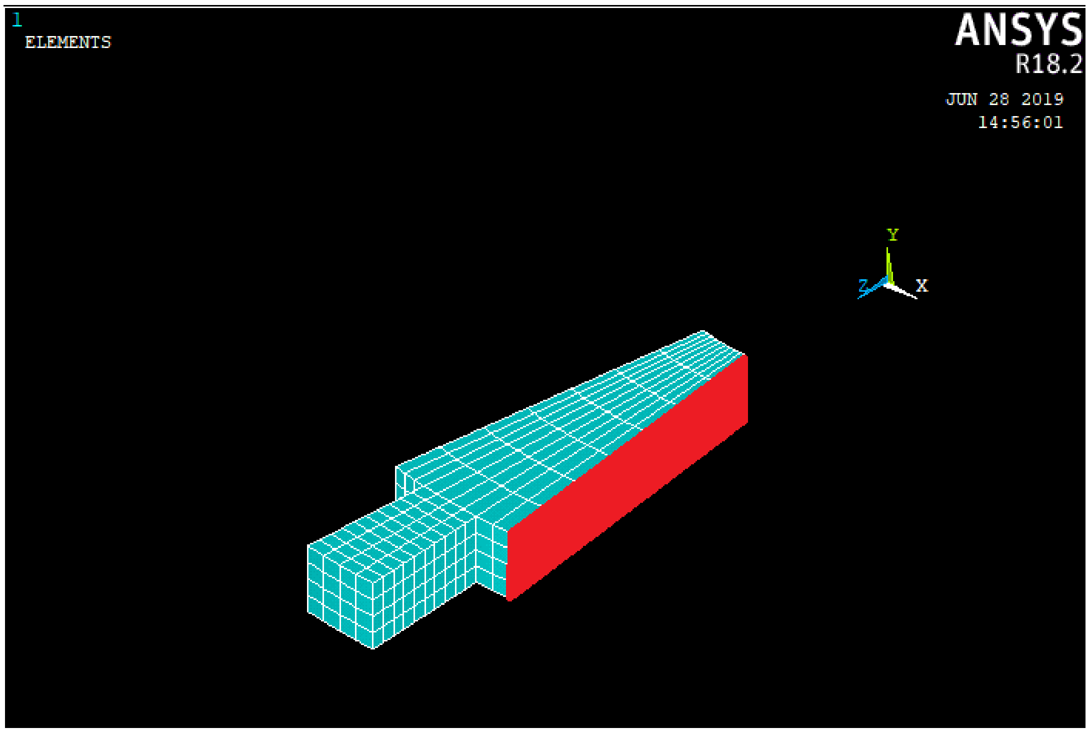

Figure 4.1.3: Group of nodes of the left face of contact or left interface

The third group, is a single node on the surface of contact between gas and blade. In this node will be applied the external force (F). In the opposite face of the blade is then chosen another node opposite to the one where the external force is applied. On this last node the reaction force (R) will be applied.
In the following picture, Figure 4.1.4 it's specified where the external force node and his reaction node are positioned. In Figure 4.1.3 it was shown the group of nodes of the left contact face.

The same will be for the nodes of the right contact faces.

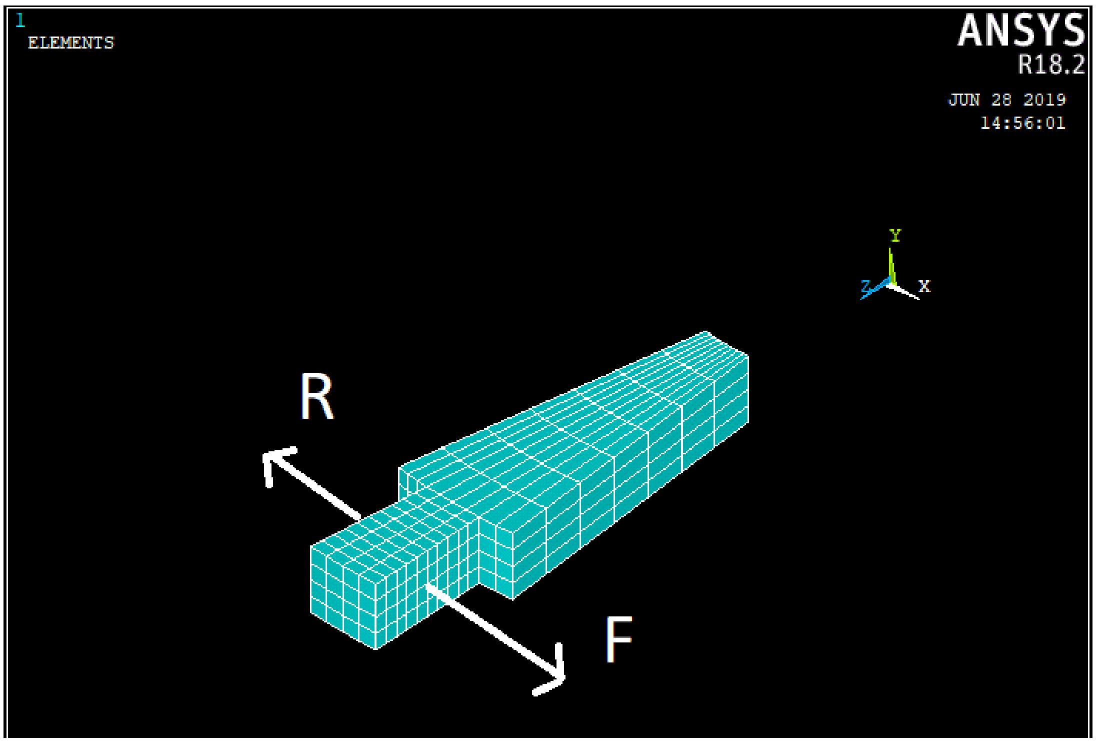

Figure 4.1.4: Position of the external force and reaction force on the surfaces of contact between gas flow and blade

The total number of nodes in this first simplified model is 100. They are 45 for the left contact face, 45 for the right contact face, 2 respectively for the external force (F) and reaction (R) and 8 for the shape modes. For this reason, since the degrees of freedom (DoF's) for each node are three, the matixes have a dimension equal to 300×300. To make the following steps more understandable this model in the following pages will be called "First reduced model". In the following chapters several reduction procedures are evaluated to find the one that can give the most accurate results.
In the appendices is dedicated a part to explain more how the Full model on ANSYS was developed. In this part is also developed an explanation through images of the frequencies obtained and the displacements for each shape mode.

4.2 Comparison of the frequencies of the "First reduced model" with the "Full model" (FM) considering only one sector

The aim of this chapter is to compare the First reduced model (FRM), where only four groups of nodes where kept, and the full model (FM) considering only one sector of the rotor wheel. For the full model (FM) the results were obtained directly from ANSYS. For the First reduced model (FRM) a script on MatLab was developed to extract the reduced matrices of stiffnes and mass. These matrixes, as already said, have dimension 300×300.

A comparison between the "First reduced model" (FRM) developed on Matlab and the "Full model" (FM) on ANSYS is done. This comparison is done for the frequency of the first shape modes.
In the following table, table 4.2.1, is possible to see this comparison.

Frequencies of FM [Hz]	Frequencies of FRM [Hz]	Percentage error
0	0	...
0	0	...
0	0	...
0	0	...
0	0	...
0	0	...
1394.82	1395.17	2.4939e-4
1872.16	1873.21	5.574e-4
3190.11	3195.2919	1.626e-3
3221.1	3228.654	2.3461e-3
3535.74	3548.96	3.738e-3
4710.53	4724.76	3.02e-3
5069.76	5080.104	2.04e-3
5694.31	5080.104	3.782e-3
6305.58	6370.03	0.01
...	...	...

Table 4.2.1: Comparison of the calculated frequencies between the Full model and the First reduced model with percentage error considering only one sector

Thanks to table 4.2.1 it's possible to notice that even by studying the sector with the First reduced model (FRM) it's possible to obtain a good approximation of the results for one sector. The error between the results obtained from the two methods is very small. With this comparison was possible to understand that even with a reduced model is possible to study a system with the advantage that the quantity of DoF's that must be managed is smaller and simpler. In the next paragraph the process of assembly is developed so it will be possible to compare the results for all the 24 sectors.

4.3 Assembly process of the stiffness matrix and the mass matrix for two sectors of the First reduce model (FRM)

The final goal of this section is to built the First reduced model of the disk considering all the sectors. Previously this comparison has been done with only one sector. Now a proof that this method works even with two sectors is done. It will be done even with three and all sectors. In Figure 4.3.1 it's shown the two sectors assembly.

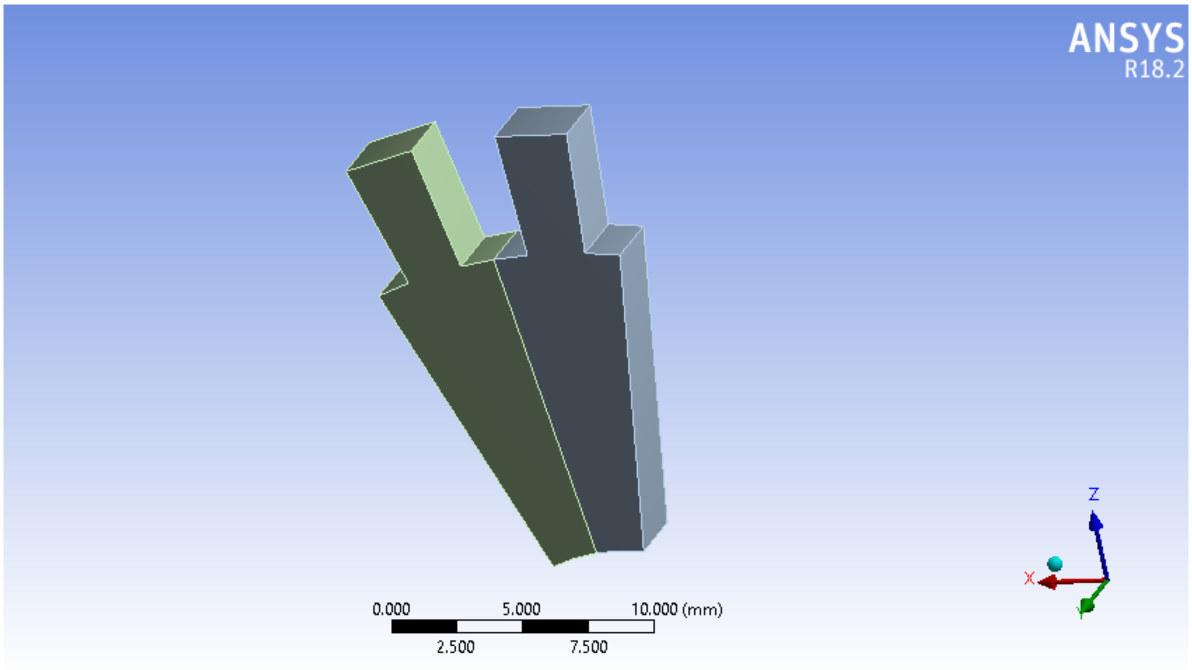

Figure 4.3.1: Assembly of two sectors of the First reduced model (FRM)

In the following table it's possible to see a comparison as done for one sector between the First reduced model (FRM) and the Full model (FM).In this case, the comparison is done for two sectors assembled.

Frequencies of FM [Hz]	Frequencies of FRM [Hz]	Percentage error
0	0	0
0	0	0
0	0	0
0	0	0
0	0	0
0	0	0
1218.65	1219.564	7.525×10^{-4}
1404.02	1404.462	3.153×10^{-4}
1526.43	1529.08774	1.74×10^{-3}
2191.65	2195	1.53×10^{-3}
2773.6	2776.985	1.22×10^{-3}
3181.57	3184.92	1.05×10^{-3}
3213.51	3219.135	1.75×10^{-3}
3999.02	4003.2537	1.059×10^{-3}
4006.29	4017.1678	2.715×10^{-3}
...	...	...

Table 4.3.1: Comparison of the calculated frequencies between the Full model and the First reduced model with percentage error considering two sectors

4.4 Assembling process of the stiffness matrix and the mass matrix for three sectors of the First reduce model (FRM)

As done for two sectors the same will be done with three sectors as shown in Figure 4.4.1.

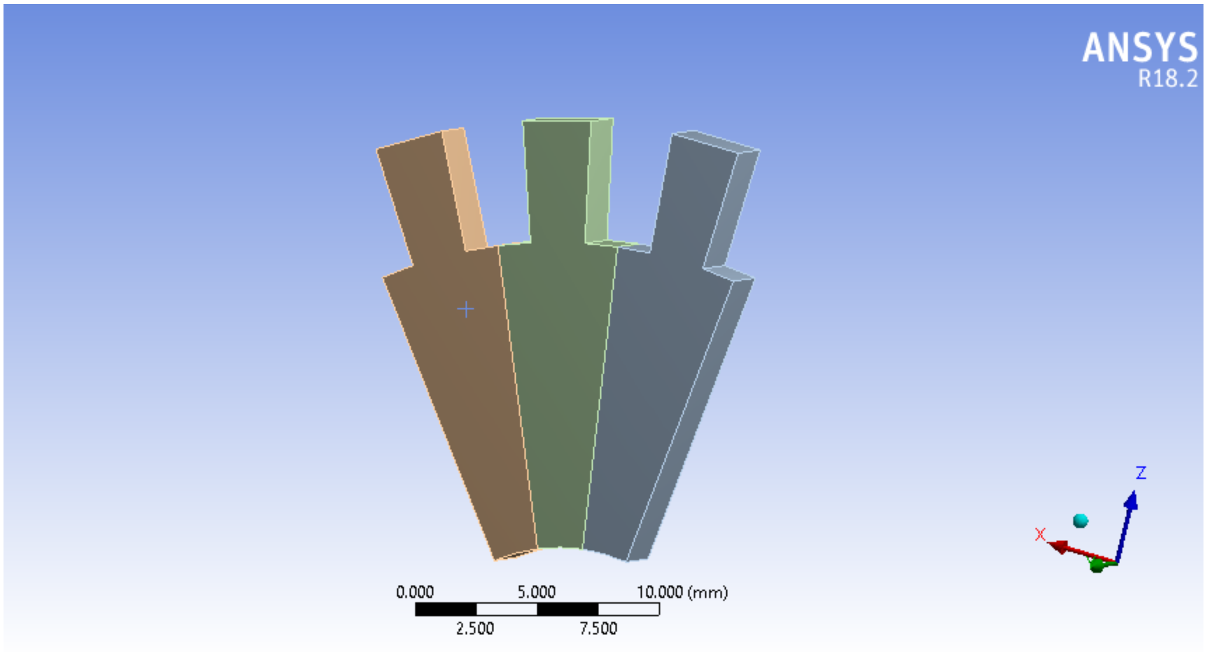

Figure 4.4.1: Assembly of three sectors

And the same for the comparison of the frequencies obtained with the Full model (FM) and the First reduced model (FRM).

Frequencies of FM [Hz]	Frequencies of FRM [Hz]	Percentage error
0	0	0
0	0	0
0	0	0
0	0	0
0	0	0
0	0	0
1040.58	1041.2431	6.38×10^{-4}
1050.22	1051.1095	8.43×10^{-4}
1422.93	1423.5	4×10^{-4}
1473.65	1475.898	1.52×10^{-3}
1577.66	1581.518	2.44×10^{-3}
2171.35	2175.71	2×10^{-3}
2398.87	2401.307	1.01×10^{-3}
2412.22	2415.35	1.29×10^{-3}
3234.06	3239.785	1.76×10^{-3}
...	...	...

Table 4.4.1: Comparison of the calculated frequencies between the Full model and the First reduced model with percentage error considering only three sectors

4.5 Assembling process of the stiffness matrix and the mass matrix for all the sectors of the First reduce model

In this last step is studied the First reduced model (FRM) considering all the 24 sectors. In the following figure it's shown the bladed disk studied.

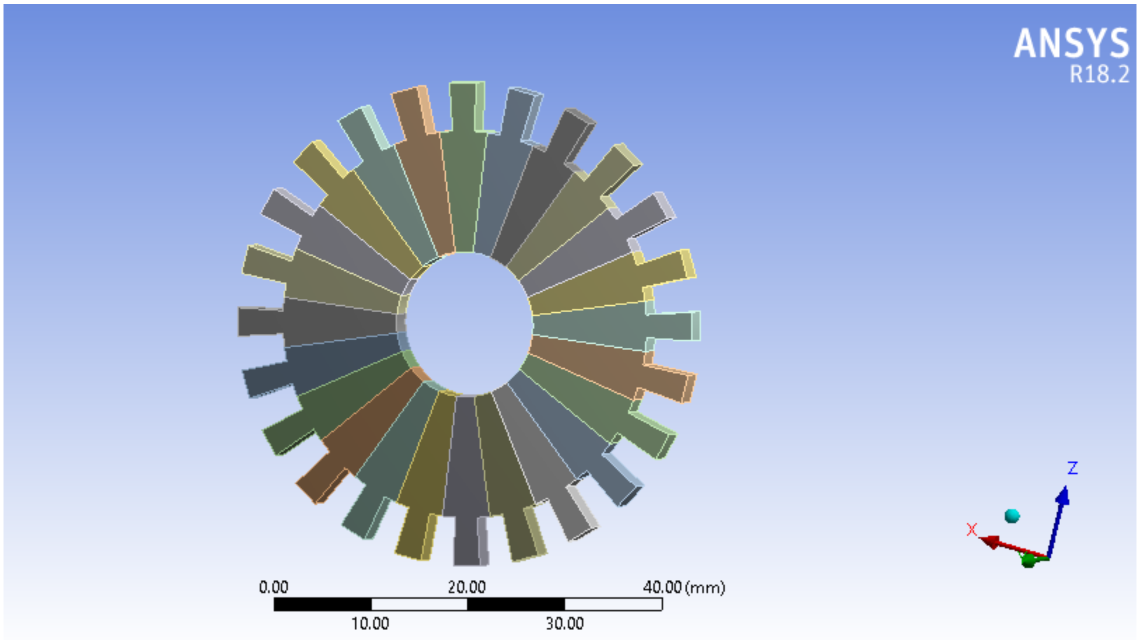

Figure 4.5.1: Assembly of all sectors

And the same for the comparison of the frequencies obtained with the Full model (FM) and the First reduced model (FRM).

Frequencies of FM [Hz]	Frequencies of FRM [Hz]	Percentage error
0	0	0
0	0	0
0	0	0
0	0	0
0	0	0
0	0	0
161.0263	161.15	7.65×10^{-4}
161.0263	161.0263	7.65×10^{-4}
283.431	283.7195	1.01×10^{-3}
366.7925	367.0455	6.89×10^{-4}
366.7925	367.0455	6.89×10^{-4}
570.28	570.6	5.54×10^{-4}
570.28	570.6	5.54×10^{-4}
570.63	571.107	8.3×10^{-4}
570.63	571.107	8.3×10^{-4}
...	...	...

Table 4.5.1: Comparison of the calculated frequencies between the Full model and the First reduced model with percentage error considering all the sectors

5 Reduction of the nodes on the interfaces of the sector

In the First reduced model evaluated previously, the number of nodes for each interface was 45. From the Full model to the First reduced model (FRM) already one step of reduction was developed.
In the following chapters some methods of reduction of the number of nodes on the interfaces of the sector will be done. The first reduction it's called "System equivalent expansion reduction process" (SEREP). This method hypothetically is able to reduce furthermore the number of nodes on the interfaces of the sector without affecting too much the results.

The second reduction called "Four-noded rectangular element reduction" consists to keep only four nodes on every interface of the sector. This means that the total number of nodes for one sector will be 18 and respectively 54 degrees of freedom (DoF's). The further reductions respectively called "Eight-noded rectangular reduction" and "Nine-noded rectangular reduction" consist in keeping respectively 8 and 9 nodes on every interface of the sector. The results then will be compared with the Full model both for the sector and for the complete disk assembled.

5.1 Reduction with SEREP

In this method it's possible to calculate the eigenmodes and eigenfrequencies of the original model. As it's possible to see, in the following formula the displacements {x} are divided in master and slave. The first one are active and the second one are omissive. ψ and q represent respectively the modal matrix and the vector of modal coordinates.

$$x = \begin{pmatrix} x_m \\ x_s \end{pmatrix} = \begin{pmatrix} \psi_m \\ \psi_s \end{pmatrix} q$$

$$\begin{pmatrix} x_m \\ x_s \end{pmatrix} = \begin{pmatrix} \psi_m \\ \psi_s \end{pmatrix} (\psi_m)^+ x_m = T_{SEREP} x_m$$

In the previous formula $(\psi_m)^+$ represents the pseudo-inversion of ψ_m. First, a verification of the efficiency of this method on a simple beam is done. The beam considered is shown in Figure 5.1.1.

Figure 5.1.1: Model of a simple beam

It's possible to see in Figure 5.1.1 that the beam has been divided in small elements. The number of elements in this case is 19 with 20 nodes. Every node has 3 degrees of freedoms Dof's so the total number of DoF's is 60. To simplify the model, the hypothesis that each element has the same properties is done. To give then, to this model the characteristics of a cantilever beam it's necessary to fix the constrains. This means that all the three DoF's of the firs node are blocked. In this case rotation and the two 2-D translations along the axis are fixed. Since this method with the equations above was not able to aproximate the results properly, the decision to try with other reduction methods was taken. These methods use the Polynomial Series.

5.2 Four-noded rectangular element reduction

Since the SEREP method didn't work a new method had to be studied. This method, as the SEREP method, splits the nodes in master nodes and omissive nodes. As did before the sector of the disk is consider as shown in Figure 5.2.1. In the further steps of this method both the left and the right

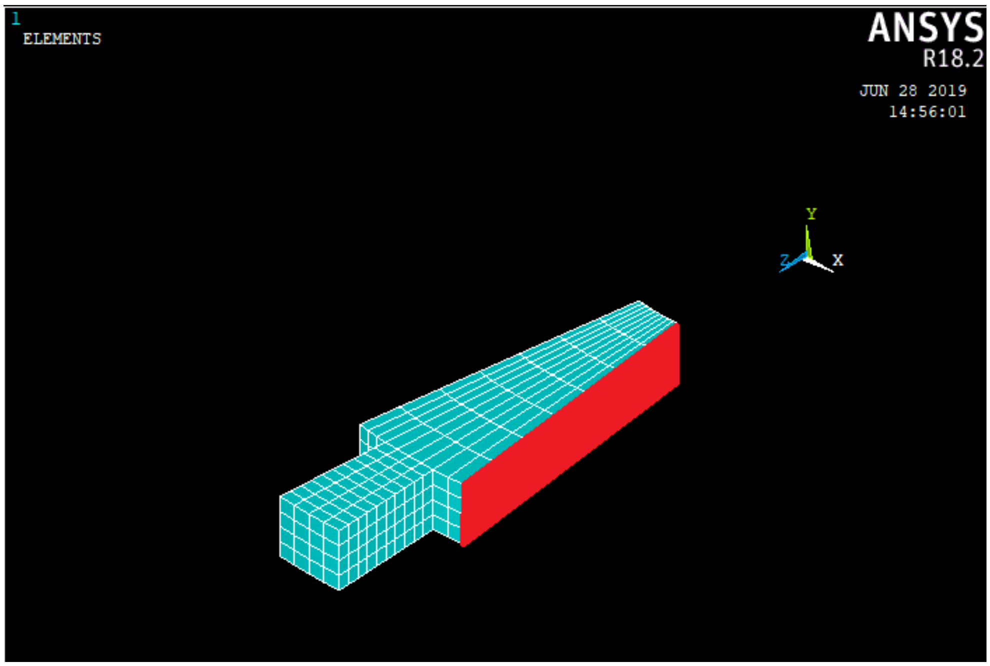

Figure 5.2.1: Left interface of the disk's sector

interface of the disk's sector are considered. To simplify the explanation in the further steps only the left interface is considered but the same steps are done also for the right interface. The left interface, as visible in Figure 5.2.1 it's the face with the x-axis positive. The distribution of nodes of the left interface for the First reduced system is shown in Figure 5.2.2.

Figure 5.2.2: Left interface of the disk's sector with reference system and number of nodes

To make the Four-noded reduction it's important to focus on the four nodes at the vertices of the face. In particular these nodes have the number 39, 44, 53 and 55. These four nodes will be the master nodes. Since there is a total of 45 nodes on the face, the other 41 nodes are all omissive nodes. In Figure 5.2.3 it's possible to see the four master nodes (nodes at the four vertices).

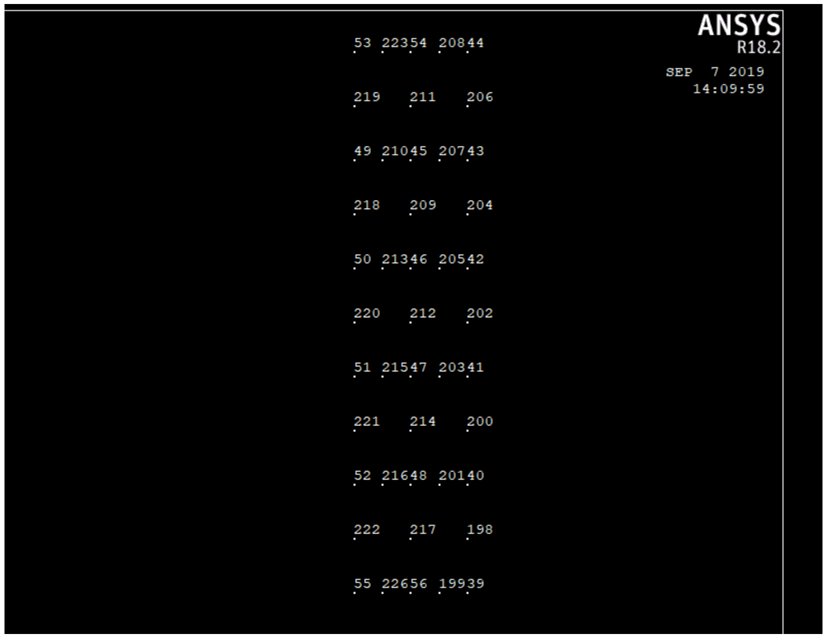

Figure 5.2.3: Left face of the disk's sector with number of nodes

To simplify the study of this method, two new transformation coordinates are introduced. These coordinates are the following:

$$\epsilon = \frac{y}{a};$$

$$\eta = \frac{z}{b};$$

With (a) and (b) the length of respectively the short and the long side of the interface. (y) and (z) are respectively the general coordinate of the short and the long side of the interface. In Figure 5.2.4 it's shown the left interface in the new transformation coordinates and the position of the four master nodes. These coordinates η and ϵ go from zero to one. It's important to say that the same procedure has been done for the right interface also.

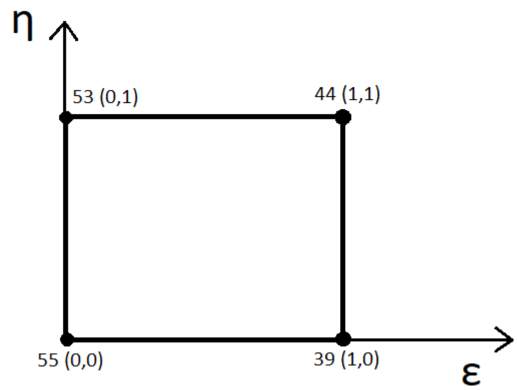

Figure 5.2.4: Transformation of the left interface of the disk's sector on the new coordinates system

In order to connect the omissive nodes that are the one not positioned at the vertices of the rectangle and the master nodes, it's necessary to calculate for each omissive node the form functions. In this case the form functions will be four because four master nodes are considered. These functions are respectively N_1, N_2, N_3 and N_4 and they are the following:

$$N_1 = \epsilon(1 - \eta)$$

$$N_2 = \epsilon\eta$$

$$N_3 = (1 - \epsilon)\eta$$

$$N_4 = (1 - \epsilon)(1 - \eta)$$

In this manner N_1 will be equal to 1 on the node number 39 and zero in all the other nodes. N_2 will be equal to 1 in the node number 44 and zero in all the others. This will be the same for the other two functions. In the following Figures are shown the four form functions.

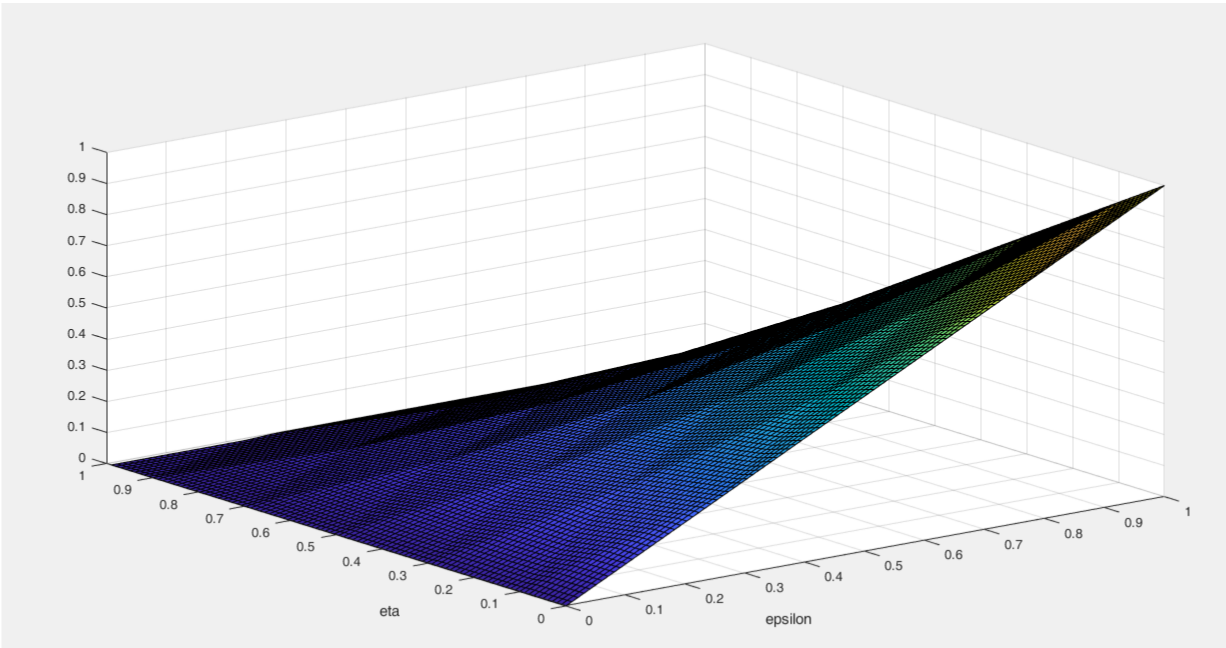

Figure 5.2.5: Form function N1

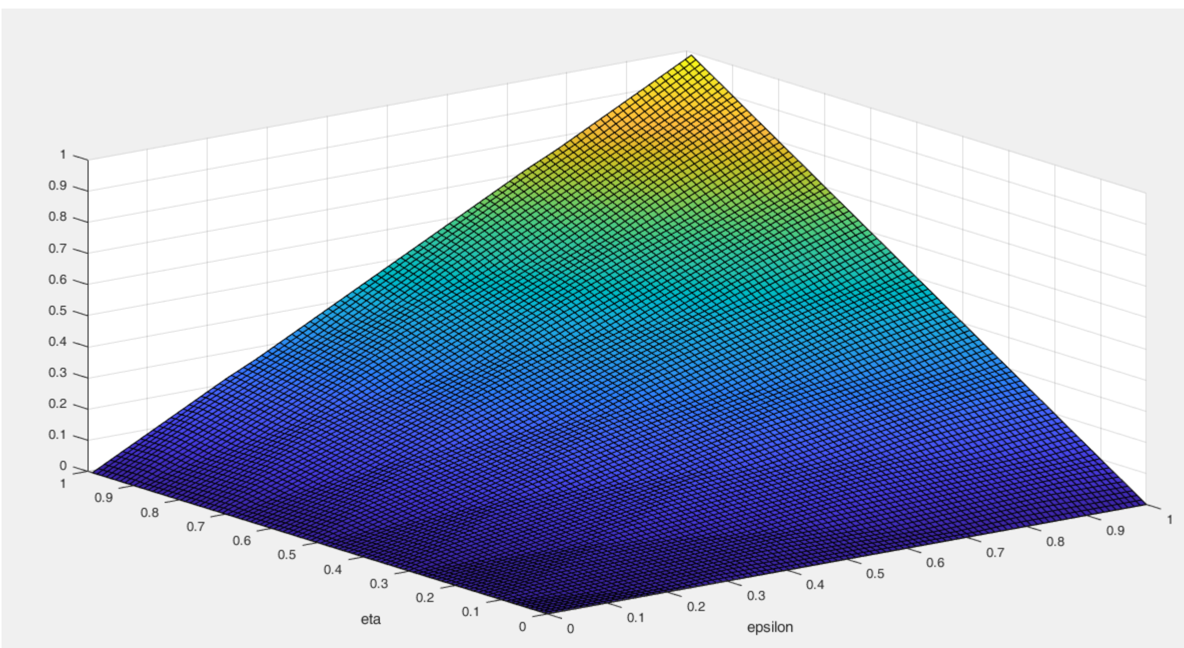

Figure 5.2.6: Form function N2

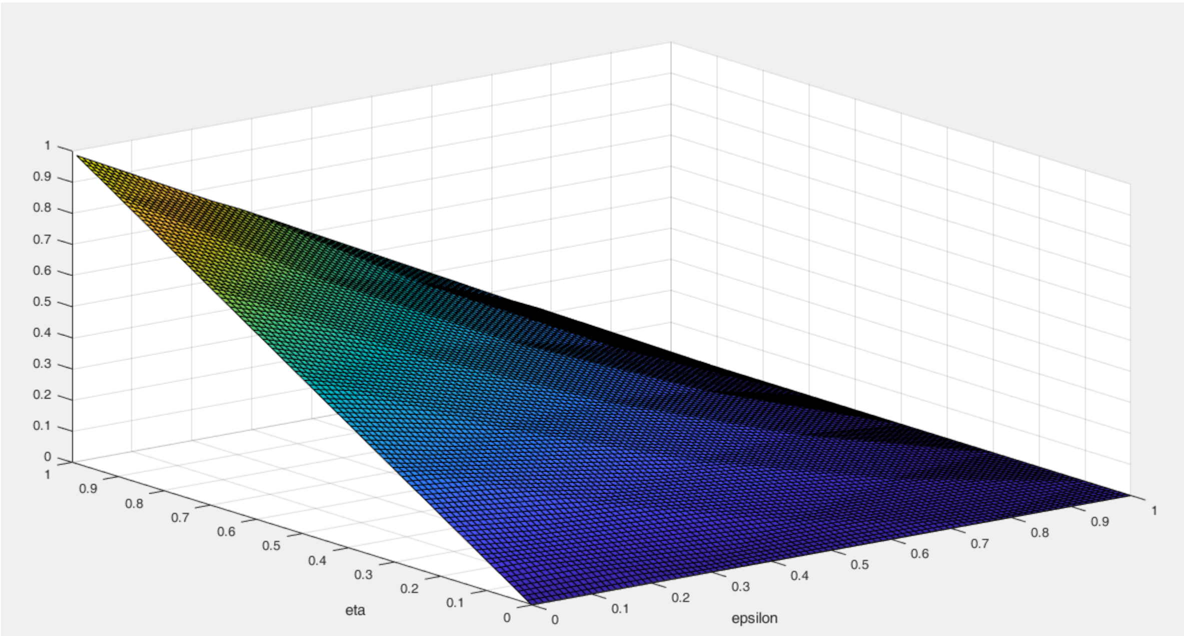

Figure 5.2.7: Form function N3

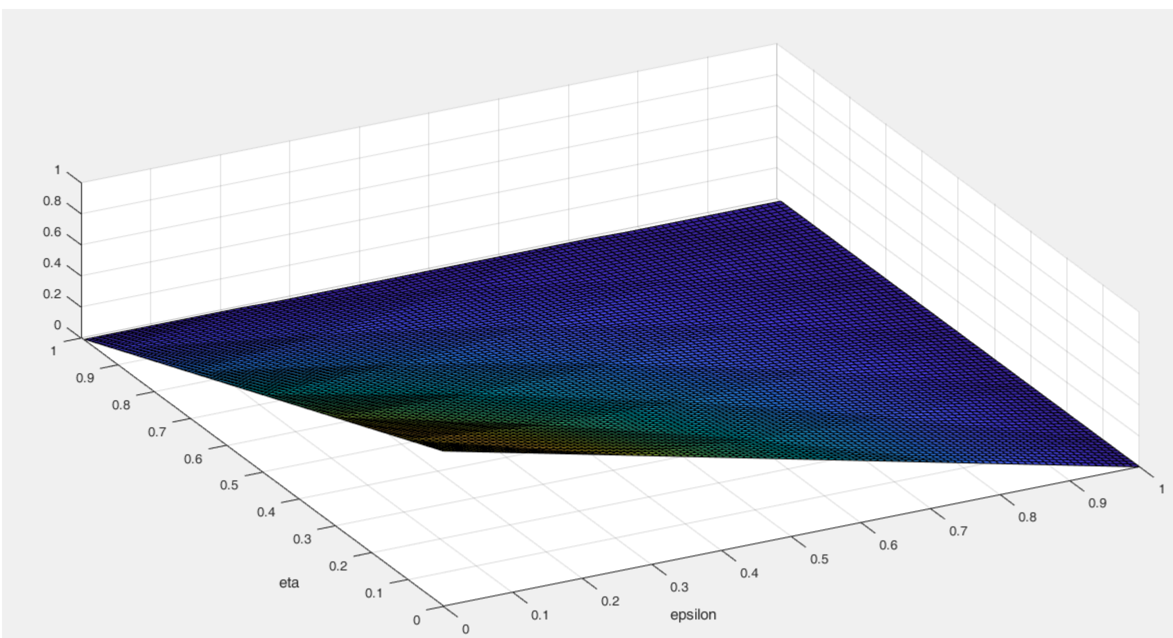

Figure 5.2.8: Form function N4

At this point it's necessary to built a transformation matrix that will connect, through the form functions (N), all the omissive nodes to the master nodes. It's necessary to remember that in each interface of the sector of the disk there are 45 nodes. These nodes are visible in Figure 5.2.3.
In the following steps the goal is to build the transformation matrix [T]. This matrix it's necessary to connect the nodes that are kept (master nodes) with all the nodes of the sector of the First reduced model(FRM). The general equation is the following:

$$x = \begin{bmatrix} All \\ the \\ DoF's \\ of \\ the \\ sector \end{bmatrix} = [T] \begin{bmatrix} All \\ the \\ DoF's \\ kept \\ in \\ the \\ sector \end{bmatrix}$$

The vector $\{x\}$ is the one that comprehends all the degrees of freedom (DoF's) of the sector. From position 1 to 135 there are the (DoF's) of the left interface in the same order as generated from ANSYS. From position 136 to 270 there are all the DoF's of the right interface in the same order as generated from ANSYS. From position 271 to 273 there are the DoF's of the external force. From position 274 to 276 there are the DoF's of the reaction. From position 277 to 300 there are the DoF's of the nodal modes. In particular an example of the system of the equations for the Four-noded model (FNM) is shown as it follows.

$$x = \begin{bmatrix} u_{39} \\ v_{39} \\ z_{39} \\ u_{40} \\ v_{40} \\ z_{40} \\ \dots \\ \dots \\ \dots \\ u_{259} \\ v_{259} \\ z_{259} \\ u_{268} \\ v_{268} \\ z_{268} \\ u_{270} \\ v_{270} \\ z_{270} \\ \dots \\ \dots \\ \dots \\ u_{276} \\ v_{276} \\ z_{276} \end{bmatrix} = \begin{bmatrix} 1\ 0\ 0\ \dots\dots\dots\dots 0 \dots\dots\dots\dots \\ 0\ 1\ 0\ \dots\dots\dots\dots 0 \dots\dots\dots\dots \\ 0\ 0\ 1\ \dots\dots\dots\dots 0 \dots\dots\dots\dots \\ N_1(40)\ 0\ 0\ N_2(40)\ 0\ 0\ N_3(40)\ 0\ 0\ N_4(40)\ 0\ 0 \\ 0\ N_1(40)\ 0\ 0\ N_2(40)\ 0\ 0\ N_3(40)\ 0\ 0\ N_4(40)\ 0 \\ 0\ 0\ N_1(40)\ 0\ 0\ N_2(40)\ 0\ 0\ N_3(40)\ 0\ 0\ N_4(40) \\ \\ \dots\dots \\ \dots\dots \\ \dots\dots \\ \\ N_1(41)\ 0\ 0\ N_2(41)\ 0\ 0\ N_3(41)\ 0\ 0\ N_4(41)\ 0\ 0 \\ 0\ N_1(41)\ 0\ 0\ N_2(41)\ 0\ 0\ N_3(41)\ 0\ 0\ N_4(41)\ 0 \\ 0\ 0\ N_1(41)\ 0\ 0\ N_2(41)\ 0\ 0\ N_3(41)\ 0\ 0\ N_4(41) \\ \dots\dots \\ \dots\dots \\ \dots\dots \\ I[30,30] \end{bmatrix} \begin{bmatrix} u_{39} \\ v_{39} \\ z_{39} \\ u_{44} \\ v_{44} \\ z_{44} \\ u_{53} \\ v_{53} \\ z_{53} \\ u_{55} \\ v_{55} \\ z_{55} \\ u_{31} \\ v_{31} \\ z_{31} \\ u_{37} \\ v_{37} \\ z_{37} \\ u_{61} \\ v_{61} \\ z_{61} \\ u_{71} \\ v_{71} \\ z_{71} \\ u_{259} \\ v_{259} \\ z_{259} \\ u_{268} \\ v_{268} \\ z_{268} \\ u_{270} \\ v_{270} \\ z_{270} \\ \dots \\ \dots \\ \dots \\ u_{276} \\ v_{276} \\ z_{276} \end{bmatrix}$$

To built the transformation matrix [T] it's necessary to keep the following relations:

- for all the DoF's of the master nodes of the both interfaces, in this case node number (39, 44, 53, 55) for the left interface and (37, 31, 61, 71) for the right face, the equation must be $u_{39} = u_{39}$, $v_{39} = v_{39}$ and so on.
- for all the DoF's of the omissive nodes the equation should be $u_{40} = N_1(40)u_{39}+N_2(40)u_{44}+N_3(40)u_{53}+N_4(40)u_{55}$, $v_{40} = N_1(40)v_{39}+N_2(40)v_{44}+N_3(40)v_{53} + N_4(40)v_{55}$ and so on.
- for all the DoF's of the force (259) and reaction (268) and the shape modes (from 270 to 276) the equation should be $u_{259} = u_{259}$, $v_{259} = v_{259}$ and so on.

The position of the identity matrixes and the form functions (N) is determined from the order of the degrees of freedom (DoF's) chosen in the vector of the nodes kept. Once the transformation matrix [T] it's calculated it's possible to proceed with the calculation of the frequencies. First it's necessary to calculate the reduced mass matrix $[M_{red}]$ and the reduced stiffness matrix $[K_{red}]$. These are the equation that allow to calculate them:

$$[K_{red}] = [T]^T[K][T]$$

$$[M_{red}] = [T]^T[M][T]$$

Where [K] and [M] are respectively the stiffness and mass matrixes of the First reduced model (FRM). The comparison of the frequencies between the First reduced model (FRM) and the Four-Noded model (FNM) is done in the following table.

Frequencies of FRM [Hz]	Frequencies of FNM [Hz]	Percentage error
0	0	0
0	0	0
0	0	0
0	0	0
0	0	0
0	0	0
1395.17	20135	45.87
1873.21	2423	29.36
3195.2919	3870	21.13
3228.654	5200	61
3548.96	5507	55.17
4724.76	6666	41.1
5080.104	8285	63.1
5080.104	9938	73.86
6370.03	10456	64.15
...	...	...

Table 5.2.1: Comparison of the calculated frequencies between the Full model and the Four-noded model with percentage error considering only one sector

As visible in table 5.2.1, the percentage error of this Four-Noded reduction method are too high. For this reason this method it's too approximative. In the next methods the form functions will be changed to approximate better the results. For this reason it's uselessness to continue with the assembly of all the sectors using the Four-noded model as method of reduction of the nodes on the interfaces.

5.3 Eight-noded rectangular element reduction

The steps to follow to develop the Eight-noded rectangular element reduction are similar to the ones that were followed for the Four-noded rectangular element reduction. The first step is to transform the general coordinates of the nodes created on the model generated on ANSYS in a system of coordinates that are simpler and more intuitive. The left interface of the sector of the disk in the new coordinate system have the following positions as shown in Figure 5.3.1. In this case η and ϵ go from -1 to 1.

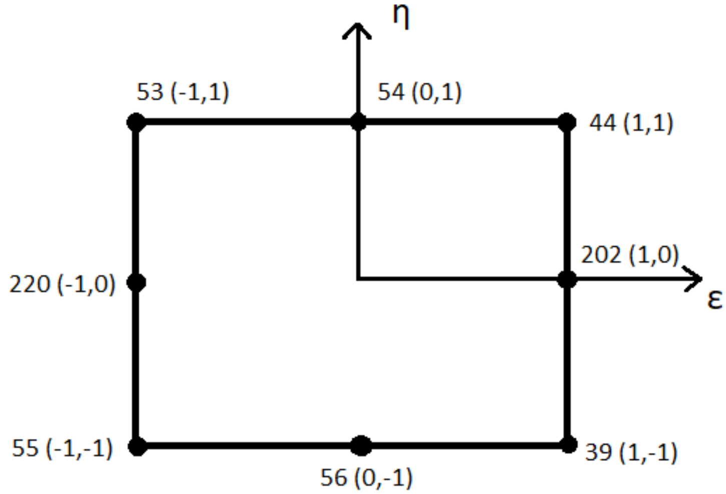

Figure 5.3.1: Transformation of the left interface of the disk's sector on the new coordinates system for the Eight-noded model (ENM)

As did previously, in order to connect the omissive nodes with the eight master nodes, the following eight form functions are introduced.

$$N_1 = (\frac{1}{4})(1+\epsilon)(1-\eta)(-1+\epsilon-\eta)$$

$$N_2 = (\frac{1}{4})(1+\epsilon)(1+\eta)(-1+\epsilon+\eta)$$

$$N_3 = (\frac{1}{4})(1-\epsilon)(1+\eta)(-1-\epsilon+\eta)$$

$$N_4 = (\frac{1}{4})(1-\epsilon)(1-\eta)(-1-\epsilon-\eta)$$

$$N_5 = (\frac{1}{2})(1+\epsilon)(1-\epsilon)(1+\eta)$$

$$N_6 = (\frac{1}{2})(1+\epsilon)(1-\epsilon)(1-\epsilon)$$

$$N_7 = (\frac{1}{2})(1+\epsilon)(1+\eta)(1-\eta)$$

$$N_8 = (\frac{1}{2})(1-\epsilon)(1-\eta)(1+\eta)$$

The property of these functions are that on one node they are equal to zero. For example N_1 is equal to one on the node 39 as shown in Figure 5.3.2.

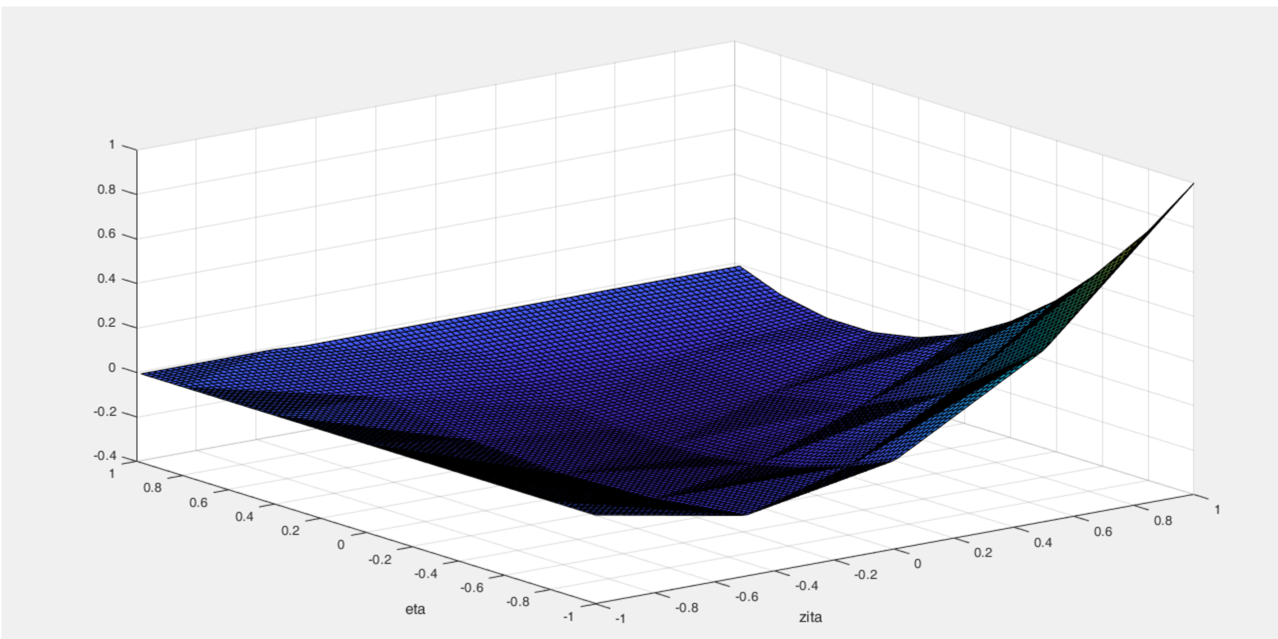

Figure 5.3.2: Form Function N_1

The Form Function N_6 is equal to one on the node 56 as shown in Figure 5.3.3. The same for the Form Function N_8 that is equal to one on the node 220 as shown in Figure 5.3.4.

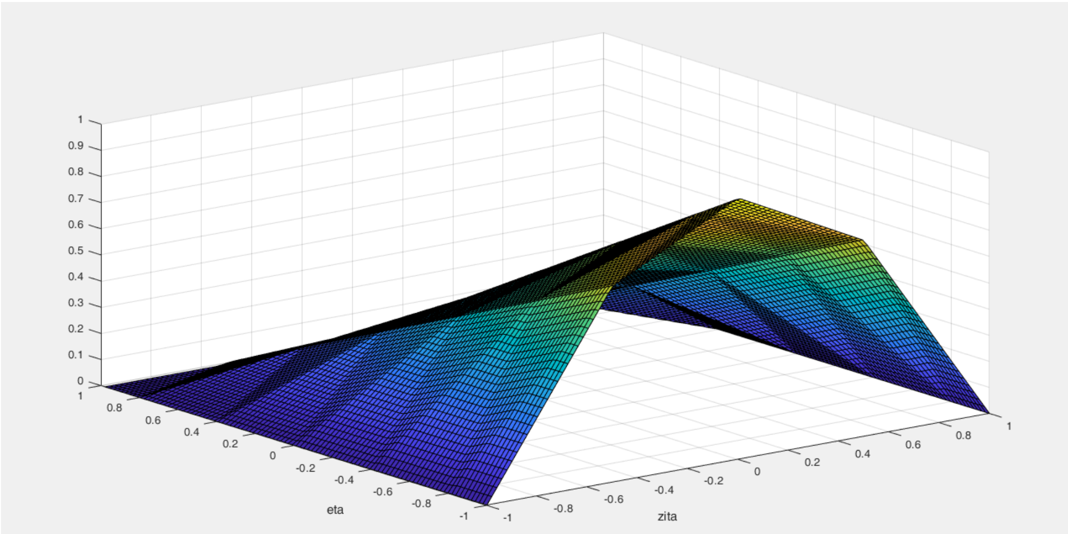

Figure 5.3.3: Form Function N_6

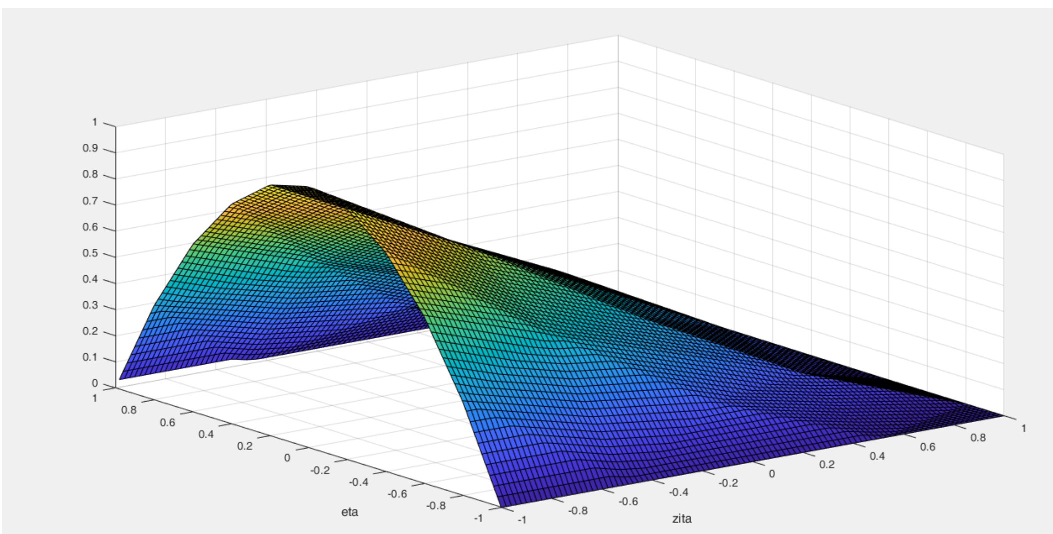

Figure 5.3.4: Form Function N_8

The next step, again is to build the transformation matrix that allows to connect the omissive nodes to the eight master nodes. Nothing changes from the Four-noded method. The only change is that instead of keeping four nodes for each interface now eight nodes are kept. The formula that connects all the degrees of freedom (DoF's) to the master nodes it's always the same:

$$x = \begin{bmatrix} All \\ the \\ DoF's \\ of \\ the \\ sector \end{bmatrix} = [T] \begin{bmatrix} All \\ the \\ DoF's \\ kept \\ in \\ the \\ sector \end{bmatrix}$$

Once again the transformation matrix [T] is obtained, the reduction of the stiffness matrix [K] and the mass matrix [M] is done at it follows:

$$[K_{red}] = [T]^T [K][T]$$

$$[M_{red}] = [T]^T [M][T]$$

The reduced stiffness matrix $[K_{red}]$ and the reduced mass matrix $[M_{red}]$ will be of dimension 78×78. The comparison between the First reduced model (FRM) and the Eight-noded model (ENM) is shown in table 5.3.1.

Frequencies of FRM [Hz]	Frequencies of ENM [Hz]	Percentage error
0	0	0
0	0	0
0	0	0
0	0	0
0	0	0
0	0	0
1395.17	1463	4.87
1873.21	1964	4.85
3195.2919	3364	5.289
3228.654	3597	11.39
3548.96	3955	11.43
4724.76	5042	6.7
5080.104	5195	2.26
5080.104	7569	32.41
6370.03	8761	37.53
...	...	...

Table 5.3.1: Comparison of the calculated frequencies between the Full model and the Eight-noded model with percentage error considering only one sector

As visible in table 5.3.1, the percentage error is smaller than in the Four-noded model. For this reason the Eight-noded model guarantees a better approximation of the results obtained for the study of one sector of the disk. Anyway, a Nine-noded reduction model has been developed to test if it is possible to reduce more the percentage error in the comparison of the results with the First reduced model (FRM).

5.4 Nine-noded rectangular element reduction

For the Nine-noded rectangular element reduction the steps will be the same as the previous. The left interface of the sector in the new coordinate system is shown in Figure 5.4.1. Even in this case η and ϵ go from -1 to 1. In this

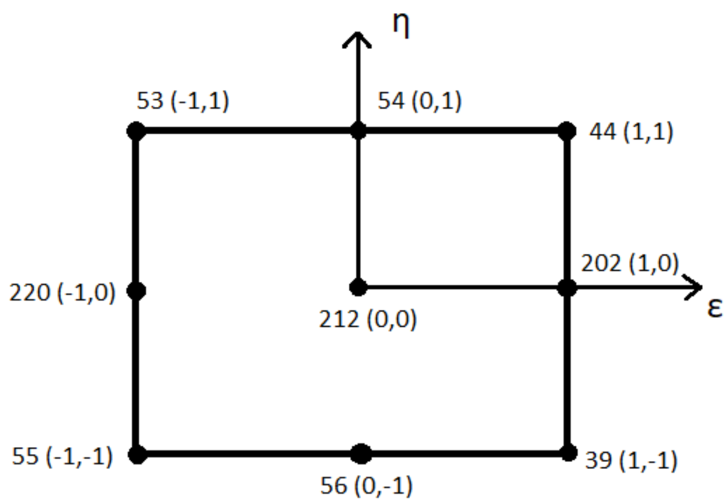

Figure 5.4.1: Transformation of the left interface of the disk's sector on the new coordinates system

case the form functions will be the followings:

$$N_1 = (-\frac{1}{2})\epsilon(1-\epsilon)(-\frac{1}{2})\eta(1-\eta)$$

$$N_2 = \frac{1}{2}\epsilon(1+\epsilon)(-\frac{1}{2})\eta(1-\eta)$$

$$N_3 = \frac{1}{2}\epsilon(1+\epsilon)\frac{1}{2}\eta(1+\eta)$$

$$N_4 = (-\frac{1}{2})\epsilon(1-\epsilon)(\frac{1}{2})\eta(1+\eta)$$

$$N_5 = (1+\epsilon)(1-\epsilon)(-\frac{1}{2})\eta(1-\eta)$$

$$N_6 = (\frac{1}{2})\epsilon(1+\epsilon)(1+\eta)(1-\eta)$$

$$N_7 = (1+\epsilon)(1-\epsilon)(\frac{1}{2})\eta(1+\eta)$$

$$N_8 = (-\frac{1}{2})\epsilon(1-\epsilon)(1+\eta)(1-\eta)$$
$$N_9 = (1+\epsilon)(1-\epsilon)(1+\eta)(1-\eta)$$

Once again the transformation matrix [T] must be generated as was done for the previous methods. Then the procedure continues with the calculation of the reduced stiffness matrix $[K_{red}]$ and the reduced mass matrix $[M_{red}]$ as it follows.

$$[K_{red}] = [T]^T[K][T]$$
$$[M_{red}] = [T]^T[M][T]$$

In this case these two matrixes have the dimension 84. It follows then the comparison in table 5.4.1 between the First reduced model (FRM) and the Nine-noded model (NNM).

Frequencies of FRM [Hz]	Frequencies of NNM [Hz]	Percentage error
0	0	0
0	0	0
0	0	0
0	0	0
0	0	0
0	0	0
1395.17	1463	4.87
1873.21	1964	4.85
3195.2919	3363	5.25
3228.654	3597	11.39
3548.96	3954	11.41
4724.76	5042	6.7
5080.104	5195	2.26
5080.104	7569	32.41
6370.03	8760	37.51
...	...	...

Table 5.4.1: Comparison of the calculated frequencies between the Full model and the Nine-noded model with percentage error considering only one sector

It's visible from the table that the results didn't change significantly from the Eight-noded model (ENM). For this reason, for the assembly process of all the 24 sectors, was decided to keep the Eight-noded model (ENM). The Eight-noded model (ENM) gives approximately the same results of the Nine-noded method (NNM) but with one node less.It's visible from the tables that the results didn't change significantly from the Eight-noded model (ENM). For this reason, for the assembly process of all the 24 sectors, was decided to keep the Eight-noded model.

6 Assembly process of the all twenty-four sectors using the Eight-noded rectangular element reduction

In the previous chapters the comparison between the frequencies of the various reduction methods have been shown. Anyway, all these comparisons were done considering the frequencies calculated for only one sector.
In this chapter is explained the assembly process of the entire disk (considering the twenty-four sectors) with the Eight-noded reduction method (ENM). The first step is to understand how the nodes between to sectors must be connected. To do so, in Figure 6.0.1 and Figure 6.0.2 are shown two sectors with the related left and right interfaces.

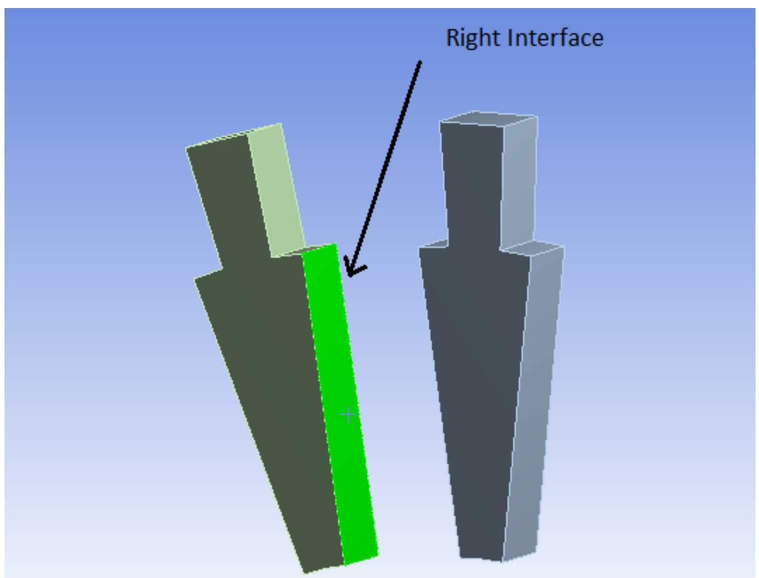

Figure 6.0.1: Right Interface of the first sector

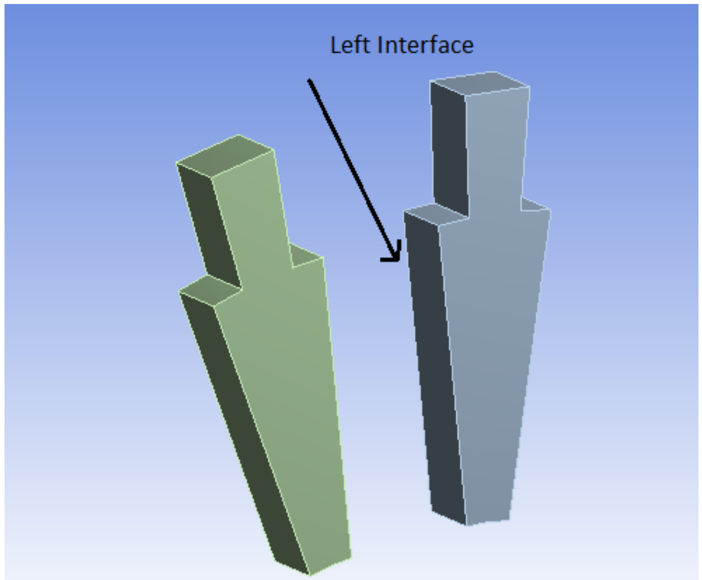

Figure 6.0.2: Left Interface of the second sector

The nodes in the new coordinate systems of the two previous interfaces are shown in Figure 6.0.3 The nodes that have the same coordinate in the

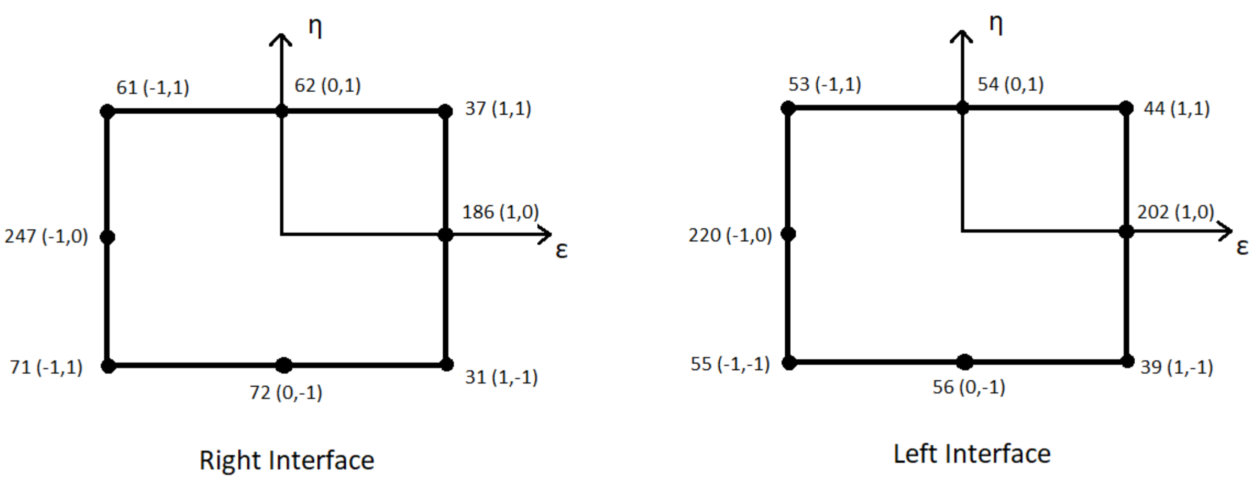

Figure 6.0.3: Left and Right Interfaces of the first and second sector

new coordinates system must be connected during the assembly process. For this reason, the node 37 must be connected with the node 44 and so on. This operation is done for all the sectors. The assembly is done clockwise, it means that the right interface of the previous sector must be assembled with the left interface of the following sector. This process goes on until the 24th sector.

After the assemblage is completed, two new matrixes have been generated. These matrixes are called global stiffness matrix $[K_{glob}]$ and the global mass matrix $[M_{glob}]$. These two matrixes are of dimension 1296×1296. This dimensions are correct since there are 54 degrees of freedom for each sector. The last step is to write a comparison table 6.0.1 of the frequencies obtained from the Eight-noded model (ENM) and the First reduced model (FRM) assembled with all 24 sectors.

Frequencies of FRM [Hz]	Frequencies of ENM [Hz]	Percentage error
0	0	0
0	0	0
0	0	0
0	0	0
0	0	0
0	0	0
161.15	150	6.91
161.15	150	6.91
283.7	280	1.3
367.0455	388	5.7
367.0455	388	5.7
570.6	570	0.10
570.6	570	0.10
571.107	628	9.96
571.107	628	9.96
...	...	...

Table 6.0.1: Comparison of the calculated frequencies between the Full model and the Eight-noded model with percentage error considering all the twenty-four sectors

7 Conclusions

Through all the methods that were developed, it's possible to have an idea on which best fit the model of a disk of a compressor for aeronautical applications. As demonstrated in the various comparisons done in the previous paragraphs, the conclusions are that the Eight-noded rectangular element reduction is the one that gives the most accurate results. Thanks to this model it was possible to reduce the number of nodes for each sector from several hundreds to eighteen. This reduction allows to calculate the frequencies with a good approximation but with a model that is lighter. As already said, this reduction is based on a system that is perfectly symmetric along the rotation axis. With the help of some "sensitivity" models, it will be possible to apply the Eight-noded rectangular element reduction to systems that are not symmetrical along the rotation axis. An example of these systems could be when the mistuning phenomenon occurs.

Appendices

A Mistuning

A.1 History and basic theory

The phenomenon of mistuning strongly affects the vibration of a rotor wheel and makes it's design more difficult. The problem of this phenomenon is that it could be generated from many causes. This makes the mistuning unpredictable. The mistuning phenomenon occurs when the rotating wheel has not a perfect symmetry a long the rotation axis. Causes of mistuning as already said, could be multiple. The most common causes could be: irregularities associated to the material properties of the blades or of the sectors of the disk, asymmetry generated during assembly, during maintenance processes or during engine's operations. The main aim of this chapter is to understand what does it means the word "mistuning" and which are the main visible differences with the results obtained from a tuned system (system without mistuning).
In general this phenomenon can be reduced but not completely eliminated. The problem of the presence of this phenomenon can have some impacts in the designing process. For an engineer, usually to perform calculations of a rotor wheel, it's more convenient to use the cyclic symmetry assumption. It was demonstrated that with this last approach the system is simplified. The problem is that this approach can be used only for symmetrical systems and a rotor wheel in which occurs the mistuned phenomenon is not. In this thesis mistuned rotor wheel are not considered. This chapter is just used as an introduction to the problems of mistuning and which differences should be expected in the results. The methods of reduction developed during the previous chapters could be then used to study a mistuned disk of compressor.

A.2 Main effects of a mistuned rotor wheel

In this section will be shown how the forced response, that was calculated in chapter three, changes with an alteration of some initial parameters. Generally, the change could affect the mass or the stiffness of some blades or some sectors of the disk. This change is very little, about 0.05% or even less. If it is very big, for example due to the lost of a blade, it's not regarding the mistuning phenomenon any-more. In this case, the change will affect the mass of some blades chosen randomly. In the previous paragraphs, was said that respectively the mass of the blade and of the slice of the disk were equal to $m_b = 0.5$ and $m_d = 1.5$ Kg. In the next steps these values are considered as standard masses. This means that this is the mass that all the blades and the slices of disk should have. In the case of a tuned system all these values are the same for each sector. For a mistuned disk this is not true any more. To generate this random variation from the standard values was decided to generate a random vector (r) of ten numbers like it follows:

0.00814723686393179
0.00905791937075619
0.00126986816293506
0.00913375856139019
0.00632359246225410
0.000975404049994095
0.00278498218867048
0.00546881519204984
0.00957506835434298
0.00964888535199277

At this point, the equation to generate the new mass values for the first ten blades was introduced as it follows:

$$m_{b,new} = m_b + m_b * r$$

Where $m_{b,new}$ is the new value of the mass of the blade and m_b is the standard value of the mass of the blade equal to $0.5Kg$. With the help of this vector it's possible to generate 6 new mass values for 6 blades. To make this study easier was decided to change the mass of the first six blades. It follows in

Figure 5.2.1 an explicative distribution of masses. It's possible to see that only the first six blades have a very small change in mass from the standard one.

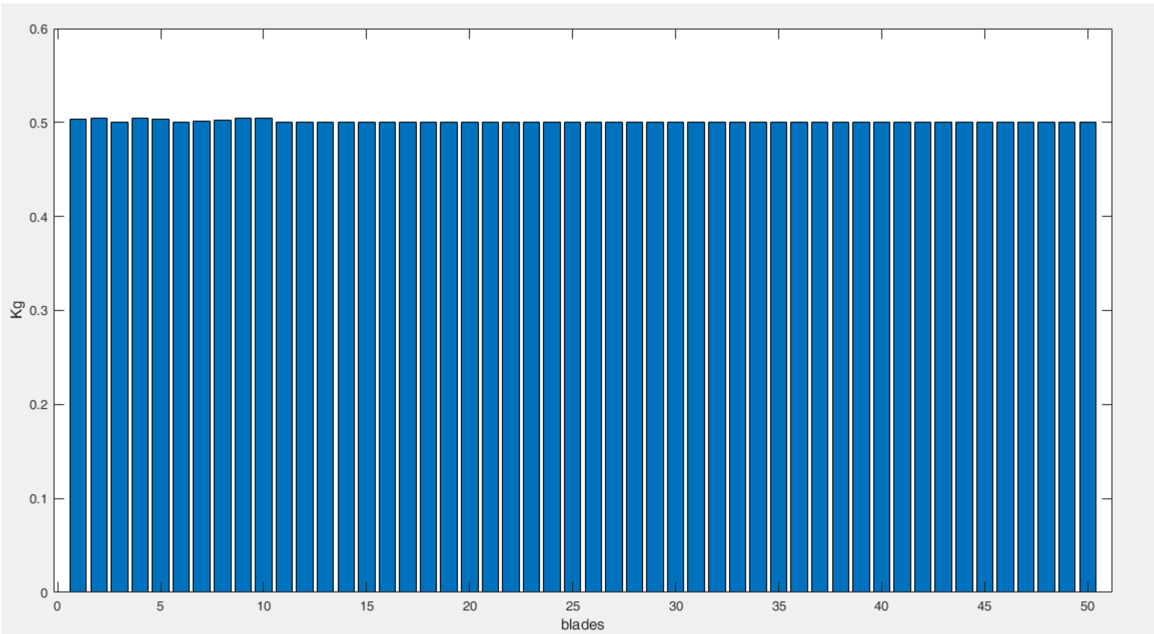

Figure A.2.1: Distribution of masses

To see the changes in the results, the graph of the forced response for the second blade and one nodal diameter is considered. The graph is shown in Figure A.2.2 In Figure A.2.2 it's possible to see that in the case of mistuned system the curve represents two tips. In the case of the tuned system, as we already studied in the previous chapters, the tip is only one. Is better to specify that in the tuned system for each shape mode corresponds two equal frequencies that makes a couple. In the table where were reported the frequencies of the first shape modes this concept was visible. For this reason, the curve that represents the tuned system has just one tip in which two frequencies are corresponding. In the curve of the mistuned system the couple of frequencies still exist, but the values are different. For this reason the tips become two. An additional example could be done for another blade. In Figure A.2.3 it's represented the blade number 10.

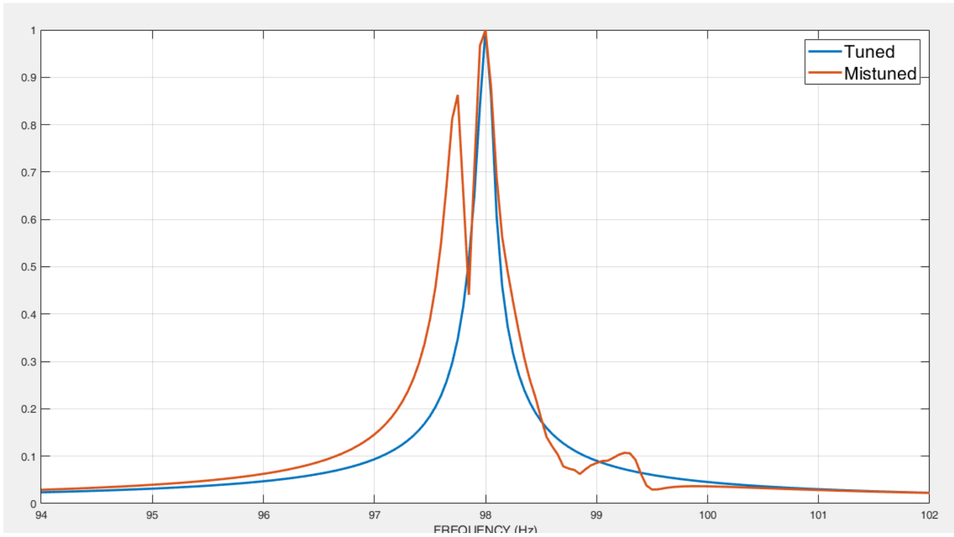

Figure A.2.2: 2nd blade comparison of the forced response diagram in the tuned and mistuned cases

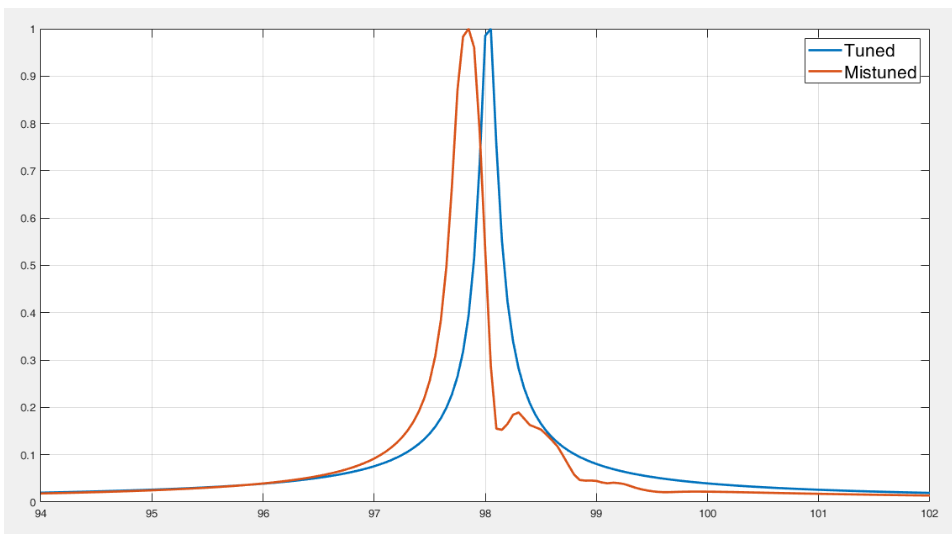

Figure A.2.3: 9th blade comparison of the forced response diagram in the tuned and mistuned cases

It follows the table of the frequencies calculated for a ”tuned” system. This table was already calculated in the previous chapters.

Frequencies [Hz]	Mode shape number
97.9893	1st shape mode
98.023	2nd shape mode
98.023	3th shape mode
98.1172	4th shape mode
98.1172	5th shape mode
98.2544	6th shape mode
98.2544	7th shape mode
98.4138	8th shape mode
98.4138	9th shape mode
98.5774	10th shape mode
98.5774	11th shape mode
98.7329	12th shape mode
98.7329	13th shape mode
...	...

It follows the table of the frequencies calculated for a "mistuned" system.

Frequencies [Hz]	Mode shape number
97.7693	1st shape mode
97.9068	2nd shape mode
98.0016	3th shape mode
98.0494	4th shape mode
98.0869	5th shape mode
98.1855	6th shape mode
98.2072	7th shape mode
98.3292	8th shape mode
98.3634	9th shape mode
98.4913	10th shape mode
98.5299	11th shape mode
98.6501	12th shape mode
98.6714	13th shape mode
...	...

By comparing these two tables it's possible to understand the concept previously explained.

B Modal Analysis of the simplified disk with twenty-four sectors

In this appendix it's explained more deeply how could be red the results obtained from a Modal Analysis. In the Chapter 1 is explained the theory that stays behind a Modal Analysis calculation. In this appendix the speech will be focused more on the results obtained from ANSYS. Previously was said that during the operations of a bladed disk some displacements from the plan in not working conditions could occur. The displacements are different from point to point. Anyway, at some particular frequencies, can occur that there are some points that don't move from the original plan of no working conditions. When this locus of points make a line, this is called "nodal diameter". In the following table the first frequencies of the modal shape analysis for the twenty-four sectors rotor wheel are reported.

Frequencies [Hz]	Mode shape number
0	1st shape mode
0	2nd shape mode
0	3th shape mode
0	4th shape mode
0	5th shape mode
0	6th shape mode
161.0263	7th shape mode
161.0263	8th shape mode
283.431	9th shape mode
366.7925	10th shape mode
366.7925	11th shape mode
570.28	12th shape mode
570.28	13th shape mode
570.63	14th shape mode
570.63	15th shape mode
...	

The first step to read the results is to understand the legend that associates the displacements to colours. This legend it's shown in Figure B.0.1.

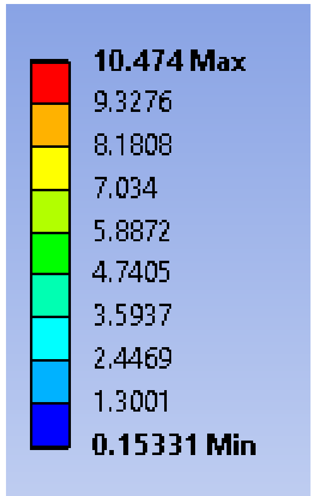

Figure B.0.1: Legend of the results generated from ANSYS for the twenty-four sectors disk

In this legend it's clear that different colours correspond to a different grade of displacement that occurs on the disk. In the table of the modal shapes it's then possible to see that the first six shape modes are equal to a frequency of 0 Hz. These six mode shapes are shown in the following Figures.

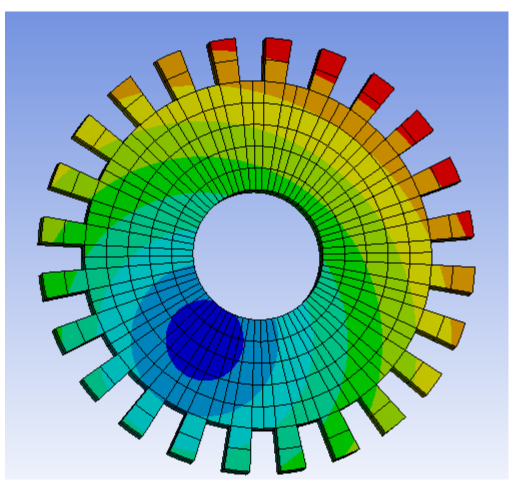

Figure B.0.2: 1st shape mode

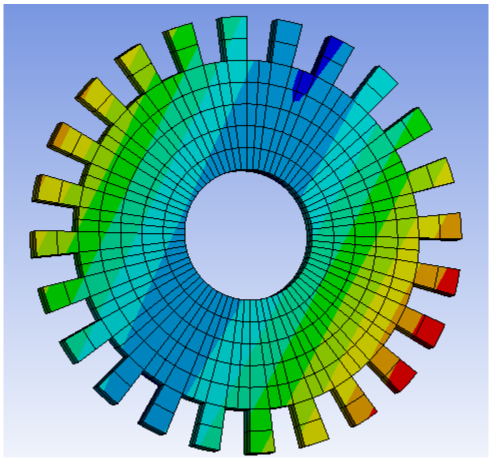

Figure B.0.3: 2nd shape mode

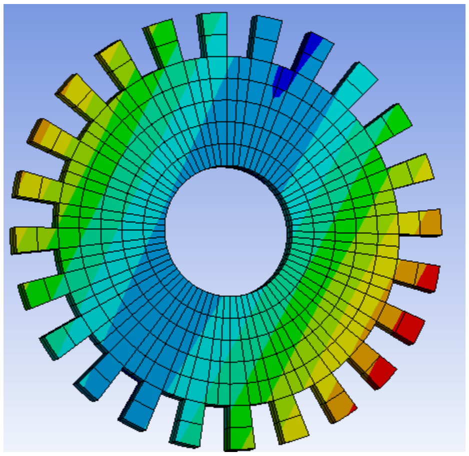

Figure B.0.4: 3rd shape mode

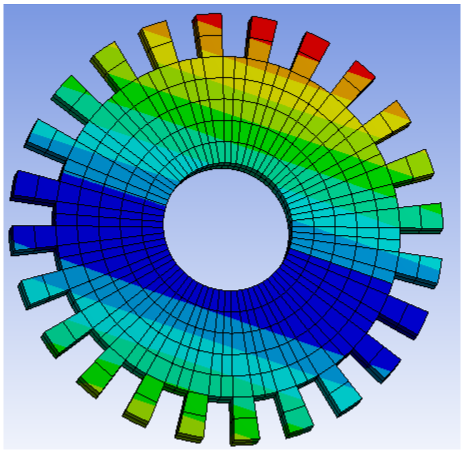

Figure B.0.5: 4th shape mode

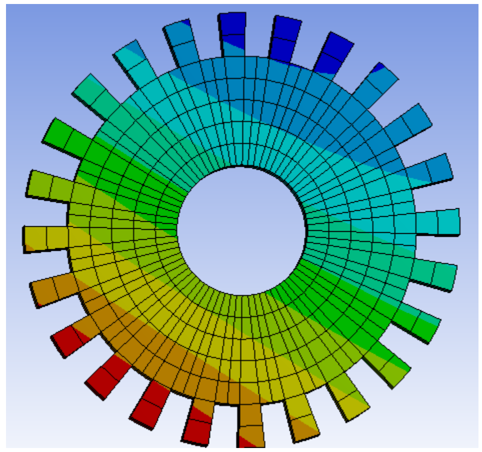

Figure B.0.6: 5th shape mode

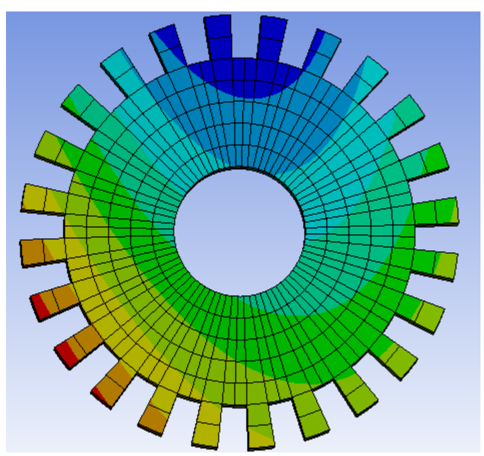

Figure B.0.7: 6th shape mode

These first six modes have the common characteristic that the displacements have no symmetry along an axis on the no working condition plan. In the next two Figures, Figure B.0.8 and Figure B.0.9, the couple of the 7th and 8th shape mode will be considered. In this case it's possible to notice that both shape modes have the same frequency and respectively two nodal diameters.

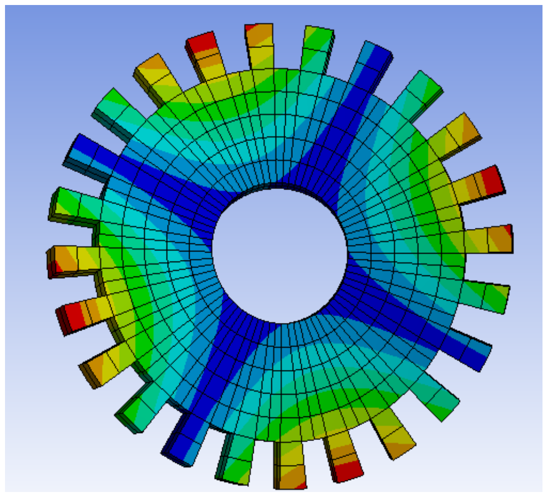

Figure B.0.8: 7th shape mode

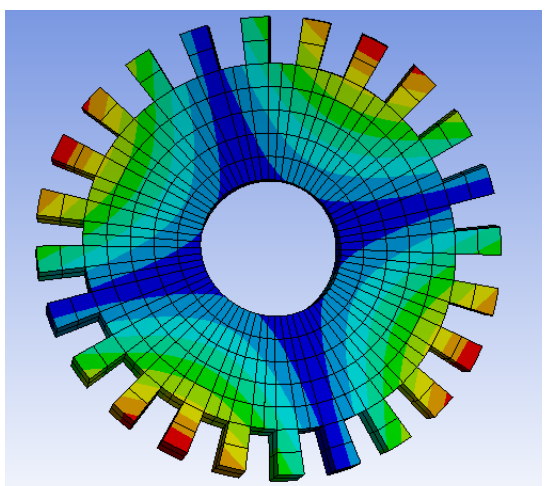

Figure B.0.9: 8th shape mode

In the 7th and 8th shape modes it's possible to see that the two nodal diameters in both cases are perpendicular to each other but their orientation it's different. As already said in Chapter 1, the phase angle (ϕ) in this case is

of 45 degrees. It means that the frequency in both cases is equal but in the 8th shape mode the nodal diameters are rotated of 45 degrees if compared with the one of the 7th shape mode.
This concept could be applied to every couple of shape modes that is reported on the table of this appendix. Between all the couples of frequencies it's possible to notice that the 9th mode shape it's a single one. The displacements of this shape mode are reported in Figure B.0.10.

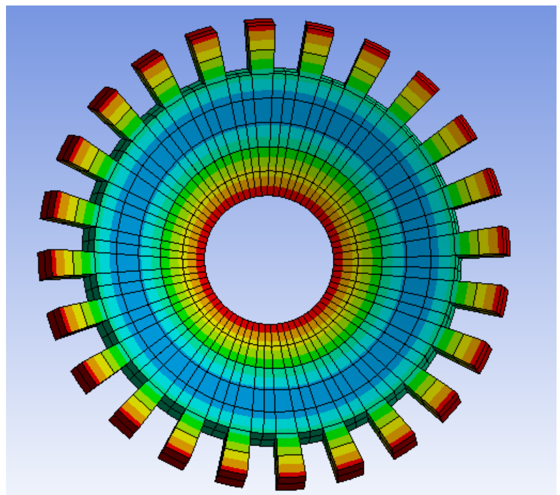

Figure B.0.10: 9th shape mode

References

[1] Richard B.Nelson, "Simplified Calculation of Eigenvector Derivatives", AIAA JOURNAL VOL.14, NO.9, 1976.

[2] P. Koutsovasilis, M. Beitelschmidt, "Comparison of model reduction techniques for large mechanical systems ", Springer Science+Business Media B.V. 2008, 2008.

[3] William C. Mills-Curran, "Calculation of Eigenvector Derivatives for Structures with Repeated Eigenvalues", AIAA JOURNAL VOL.26, NO.7, 1988.

[4] R. Lane Dailey, "Eigenvector Derivatives with Repeated Eigenvalues", AIAA JOURNAL VOL. 27, NO.4, 1989.

[5] M.I. Friswell, S.D. Garvey and J.E.T. Penny, "Model Reduction Using Dynamic and Iterated IRS Techniques", Journal of Sound and Vibration 186(2), 311-323, 1995.

[6] I.U. Ojalvo, "Efficient Computation of Modal Sensitivities for Systems with Repeated Frequencies", AIAA JOURNAL VOL.26, NO.3, 1998.

[7] Alok Sinha, "Vibration of Nearly Periodic Structures and Mistuned Bladed Rotors", 2017.

[8] S. Tiachacht, A. Bouazzouni, S. Khatir, A. Behtani, Y.-L.-M. Zhou, M. Abdel Wahab , "2774. Structural health monitorin of 3D frame structures using finite element modal analysis and genetic algorithm", Journal of Vibroengineering Vol.20,Issue I.ISSN 1392-8716 2018.

[9] D.L. Thomas , "Dynamics of Rotationally Periodic Structures", International Journal for Numerical Methods in Engineering, VOL. 14,81-102 1979.

[10] Dr.J. Dean, "Introduction o the Finite Element Method (FEM)-Lecture 1 The Direct Stiffness Method and Global Stiffness Matrix".

[11] Soo-Yeol Lee, Matthew P. Castanier and Christophe Pierre, "Assessment of Probabilistic Methods for Mistuned Bladed Disk Vibration", 46th AIAA-ASME-ASCE-AHS-ASC Structures, Structural Dynamics and Materials Conference 2005.

[12] Matthew P. Castanier and Christophe Pierre, "Modelling and Analysis of Mistuned Bladed Disk Vibration: Status and Emerging Directions", Journal of Propulsion and Power VOL. 22, NO.2 2006.

[13] Gísli Sigurbjörn Óttarsson, "Dynamic Modeling and Vibration Analysis of Mistuned Bladed Disks", A dissertation submitted in the partial fulfillment of the requirements for the degree of Doctor of Philosophy (Mechanical Engineering) in The University of Michigan 1994.

[14] Mark H. Richardson, "Modal Mass, Stiffness and Damping", Vibrant Technology, Inc. 2000.

[15] S.A Tobias and R.N. Arnold, "The Influence of Dynamical Imperfection on the Vibration of Rotating Disks", Proceedings of the Institution of Mechanical Engineers 1957 171:669 1957.

[16] Brian J. Schwarz and Mark H.Richardson, "Structural Modifications Using Higher Order Elements", 15th IMAC Conference 1997.

[17] T.P. Fries, S.Omerovic, D. Schollhammer, J. Steidl, "Higher-order meshing of implicit geometries -part I: Integration and interpolation in cut elements", Institute of Structural Analysis Graz University of Technology 2017.

[18] E. Pipitone, "Dynamics of a mistuned bladed disk and friction damping analysis", Master's Thesis, Politecnico di Torino 2018.